

# Isothermal and non-isothermal flow in street canyons: A review from theoretical, experimental and numerical perspectives

## Journal Article

**Author(s):**

Zhao, Yongling; Chew, Lup W.; Kubilay, Aytaç; Carmeliet, Jan

**Publication date:**

2020-10-15

**Permanent link:**

<https://doi.org/10.3929/ethz-b-000439889>

**Rights / license:**

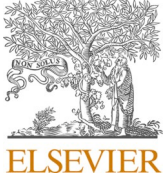
[Creative Commons Attribution 4.0 International](#)

**Originally published in:**

Building and Environment 184, <https://doi.org/10.1016/j.buildenv.2020.107163>

**Funding acknowledgement:**

169323 - Wind-driven rain impact of urban microclimate: wetting and drying processes in urban environment (SNF)



## Isothermal and non-isothermal flow in street canyons: A review from theoretical, experimental and numerical perspectives



Yongling Zhao<sup>a,\*</sup>, Lup Wai Chew<sup>b,\*\*,1</sup>, Aytaç Kubilay<sup>a</sup>, Jan Carmeliet<sup>a</sup>

<sup>a</sup> Department of Mechanical and Process Engineering, ETH Zürich, Zürich, 8093, Switzerland

<sup>b</sup> Department of Mechanical Engineering, Massachusetts Institute of Technology, 77 Massachusetts Avenue, Cambridge, MA, 02139, USA

### ARTICLE INFO

#### Keywords:

Urban street canyon flows  
Wind tunnel measurements  
Scaling analysis  
Computational fluid dynamics  
Turbulence models

### ABSTRACT

Urban street canyon flows play a central role in microclimate control, from street canyon to neighbourhood and city scale, which affect pollutant dispersion, thermal comfort of residents and building energy consumption for various indoor and outdoor flow conditioning systems. Extensive studies have been devoted to this field, from theoretical modelling to experimental measurements and numerical simulations. While some important characteristics of street canyon flows, such as the presence of a primary standing vortex and the mechanism for its establishment, have been well revealed, a holistic understanding consolidating theoretical, experimental and numerical research has not been achieved. This review is therefore aimed to holistically articulate these approaches and research outcomes in the field. Some critical points overlooked in the literature are identified and commented on. These are: distinguishing gradient and bulk Richardson numbers; identifying dominant similarity characteristic numbers for scaling down models; predicting the condition in which thermal effects come into play; modelling the convective heat transfer in non-equilibrium mixed convection conditions using wall functions; and exploring the influence of neutral and non-neutral urban boundary layers on street canyon flows and associated passive scalar dispersion. The review is concluded with an outlook to most challenging research questions towards understanding of microclimate of full-scale realistic street canyons.

### 1. Introduction

Half of the global population are living in cities and the number is projected to increase to 70% in 2050 [1]. One focal concern with city-scale climate is the urban heat island effect [2–5], which involves multi-scale and multi-disciplinary physical processes and factors, such as long-wave radiation in daytime [6–10], rain driven by wind [11–15], moisture change due to vegetation [16–20], input of anthropogenic heat [21–27], morphology of the city [28–34], building configurations [28, 29,31–34], etc. Huge efforts of the urban physics community have been devoted to various topics in recent decades and understanding of the urban heat island has advanced dramatically.

Physical processes in the urban boundary layer and canopy layer govern the urban heat island effect [3], as shown in Fig. 1. The mixing depth ( $h^*$ ) is time dependent, which can grow to 1.5–2 km in the afternoon and decreases considerably to several hundred of meters at night [3]. The mixing height and the urban heat island intensity can be

estimated by the correlations given by Ref. [35].

Among the complex physical mechanisms contributing to the urban heat island effect, street canyon flow is one of the most relevant in local thermal comfort [36–38], airborne pollutant dispersion [39–43] and ventilation around buildings [44–48]. Studies of such flows started since the 1960s and have been one of the most important research topics in the context of urban microclimate. A key feature of street canyon flows is the presence of vortex flow structures [49]. Much effort has been devoted into the understanding and manipulation of various factors affecting these vortex flow structures for desired purposes. These studies encompass thermal conditions [27,37–39,44,50–58], geometrical variations [40,42,59–65] and characteristics of local wind [66–68].

Thermal conditions of grounds, building façades and ambient surroundings directly affect the physics of street canyon flows. In addition to the Reynolds number used in the characterisation of isothermal street canyon flows, Richardson number has been widely adopted to characterise buoyancy effects of non-isothermal street canyon flows [69].

\* Corresponding author.

\*\* Corresponding author.

E-mail addresses: [yozhao@ethz.ch](mailto:yozhao@ethz.ch) (Y. Zhao), [lupwai@mit.edu](mailto:lupwai@mit.edu), [lupwai@stanford.edu](mailto:lupwai@stanford.edu) (L.W. Chew).

<sup>1</sup> Current affiliation: Stanford University.

When it comes to the definition of the critical Richardson number beyond which the incoming flow dominates the fluid dynamics, different criteria in the literature emerge [37,69,70]. Clarifications to this point will be made in section 3.

Geometrical variations of street canyons are commonly characterised by their height-to-width aspect ratios. Most studies have examined the height-to-width aspect ratio of 1 and some extended to large aspect ratios up to 10. Both the height-to-width and height-to-length aspect ratios of street canyons play an important role in the transition from “skimming” to “wake interference” and ‘isolated’ flow regimes [71]. The influence of the height-to-width aspect ratio on flow regimes is schematically shown in Fig. 1. Geometrical modifications to building roofs and ground floors have also been visited for seeking better ventilation or pollutant dispersion [57].

Local wind is commonly characterised by the Reynolds number ( $Re$ ) and turbulence intensity. Studies have examined the effects of  $Re$  extensively, covering a wide range from  $10^3$  to  $10^6$ . The strength and core centre of standing vortices in street canyons are found to be  $Re$  dependent at low  $Re$  [72] and  $Re$  independent at large  $Re$  [56]. Turbulence intensity of the incoming flow also plays an important role in the flow dynamics. Models for high turbulence intensity and low turbulence intensity scenarios have been proposed and will be discussed below.

The purpose of this review is two-fold. First, it holistically articulates existing understanding of street canyon flows from theoretical, experimental and numerical perspectives for both isothermal and non-isothermal street canyon flows. Second, it distinguishes inconsistencies, unknowns and research gaps in this topic. This review is centred on flows developed in geometrically generalised street canyons with a representative perpendicular approaching flow. The generic understanding gained through those studies in the community underpins variant studies with different scopes. Turbulent dispersion by three-dimensional street canyon flows, which is an associated physical process, is briefly reviewed. Effects of more complex street canyon geometries, non-perpendicular approaching flow and complex heterogeneous surrounding buildings on the characteristics of street canyon flows are only briefly covered.

Review of studies on isothermal street canyon flows will be elaborated in section 2 and the research of non-isothermal flows is discussed in section 3. In section 4, a discussion on roles of local buoyancy effects on street canyon flows is first made based on a scaling analysis, followed by the review on the effects of non-neutral approaching urban boundary layer on passive scalar dispersion. In section 5, emerging approaches for passive scalar dispersion by street canyon flows are briefly discussed. Concluding remarks are presented in section 6.

## 2. Advances on isothermal flows

### 2.1. Theoretical analyses

Street canyon flow is complex in a sense that the shear flow from building roofs and the inflow from lateral sides of an upstream building interact with the primary circulating flow inside the street canyon. The characteristics of the shear flow and inflow depend not only on the approaching flow, but also on the geometrical features of the buildings, like the width and roof configuration, and the length of the street canyon. The street canyon flow is typically three-dimensional and presents complex helix and coherent hairpin structures [73].

Instead of considering all these complex dynamics, cavity flow where the lateral inflow is not taken into account is a classical approximation for revealing primary fluid dynamics inside street canyons. A typical street canyon flow is featured by a primary standing vortex and associated secondary vortices at corners of a street canyon (see Fig. 2a), which can be simplified by both classical lid-driven (see Fig. 2b) and more recent shear-driven models (see Fig. 2c). It is worth noting that this assumption is valid when the canyon of interest can be classified to be a long one where vortices induced by the lateral inflow (or outflow) are confined near corners of the canyon [71]. Those simplified models usually assume the flow to be predominantly two-dimensional, and dominated by the incoming flow velocity,  $U_\infty$ , canyon width,  $W$ , and canyon height,  $H$ , see Fig. 2a. The Reynolds number is defined as  $Re = U_\infty \xi / \nu$ , where  $\nu$  is the kinematic viscosity of the fluid and  $\xi$  is a characteristic length or length scale. It is worth noting that the length scale  $\xi$  can be chosen to be the canyon width ( $W$ ) [72,75], canyon height ( $H$ ) [44,58,69] or the momentum thickness of the incoming boundary layer ( $\theta$ ) [72,75–77]. As the names of both models suggest, the presence and dynamics of the shear layer in the upper part of a cavity are only considered in the shear-driven model.

While the lid-driven model captures time-averaged characteristics of the flow, the shear-driven model is able to distinguish the different characteristic zones [74]. In case of a highly turbulent shear flow at the top of the cavity, it remains challenging to model the coherent structures that take place in the form of sweeps (entrainment) and ejections (flushing). It is therefore worthwhile to review capacities and limitations of both models. In the following sections, the Reynolds numbers calculated with a length scale of the street canyon are denoted by  $Re$  and the ones estimated using a momentum thickness of incoming boundary layers are denoted by  $Re_{mt}$ . It is worth clarifying that the momentum thickness is a measure of the reduction in momentum transport in the incoming boundary layer, which can be calculated from its vertical velocity profile.

#### 2.1.1. Lid-driven flow

The lid-driven model can be recognised as one of the earliest theo-

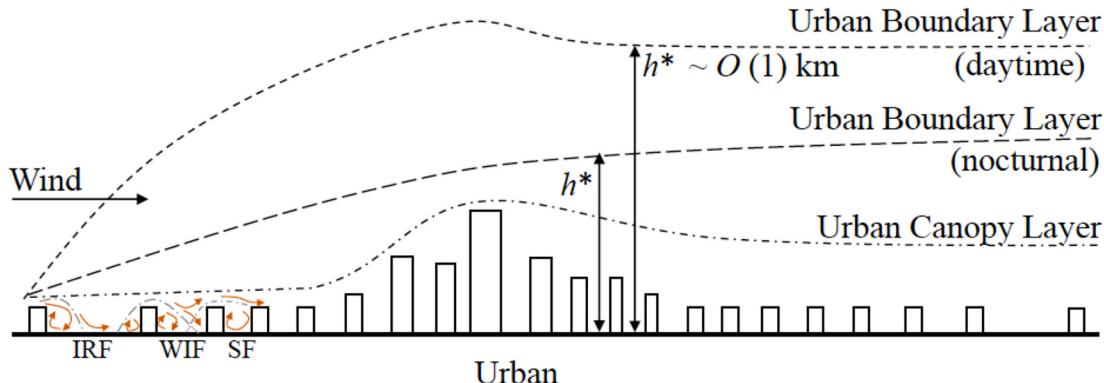


**Fig. 1.** Schematic diagram of the daytime and nocturnal urban boundary layers and canopy layer. The mixing depth denoted by  $h^*$  is larger during daytime. IRF, WIF and SF denote isolated roughness flow, wake interference flow and skimming flow, respectively.

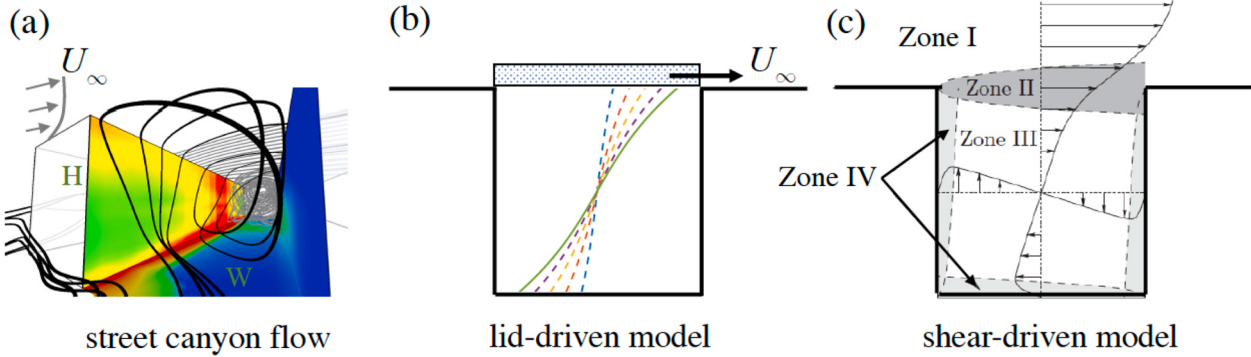


**Fig. 2.** Schematics showing (a) three-dimensional flow in a street canyon with non-isothermal building and ground surfaces based on Ref. [4], (b) velocity profiles in a lid-driven model and (c) characteristic zones in a shear-driven model [74]. Note that in (a) the colours indicate the temperature profile of surfaces, the thicker streamlines in black suggest the lateral inflow and the thin streamlines in grey depict the shear flow from the upstream building roof.

retical approximations for street canyon flows [78,79], in which the flow is characterised by the Reynolds number  $Re = U_\infty \xi / \nu$  where  $U_\infty$  is the reference velocity of the lid and  $\xi$  is the width of the cavity. The influence of cavity length on flow dynamics is not considered in the lid-driven model, which can alter the primary vortex and induces flow transition from the “skimming” to the “wake interference” regime [71]. The representative circulating flows were first discovered in Ref. [78] for  $Re = 0, 8, 32, 64$  and aspect ratio,  $A = 0.5, 1.0, 2.0$ .

The vertical velocity component,  $V$ , which indicates the strength of the vortical flow in the cavity, is derived to be:

$$\frac{1}{\Omega} \left( \frac{V}{U_\infty} \right) = \left( \frac{1}{2} - Y \right) - \frac{4}{\pi^2} \sum_{n=1}^{\infty} \frac{1}{(2n-1)^2} \operatorname{sech} \frac{(2n-1)}{2} \pi \cos(2n-1)\pi Y , \quad (1)$$

where  $\Omega = 1.886$  is the inviscid limit,  $U_\infty$  the reference velocity of the lid and  $Y$  the nondimensional height of the cavity [79]. Fig. 3 shows the profile of the vertical velocity at the mid-height of the cavity, which is estimated by Ref. [79]. Experimental results obtained in Ref. [80] for  $1000 < Re < 4000$  are included as markers. It is interesting to note that the Burggraf model predicts the velocity accurately, except for the

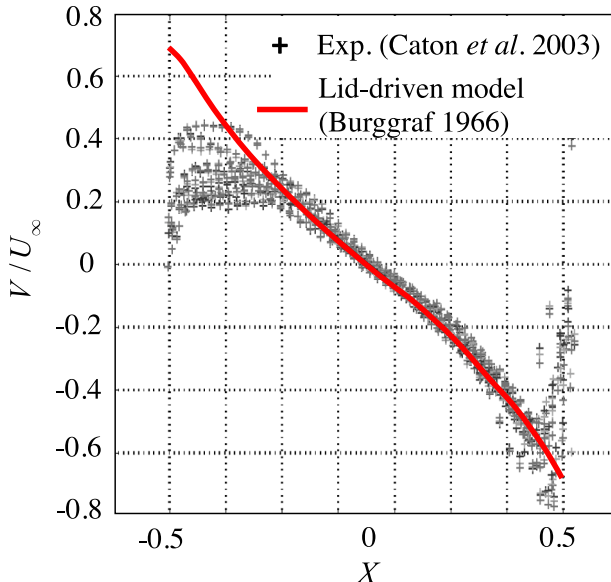


**Fig. 3.** Profiles of vertical velocity component at the mid-height of a cavity estimated by Eq. (1) and experimental results for  $1000 < Re < 4000$  [80].  $X$  denotes the width of the cavity normalised by the cavity height,  $V$  the vertical velocity and  $U_\infty$  the reference velocity.

regions close to the walls where different flow regimes are present.

The series given by Eq. (1) converges rapidly and only two or three terms ( $n$  up to 3) are needed to give considerable accuracy. Despite being a highly simplified model in which the shear flow from an upstream building roof and lateral flow at corners of the canyon are not considered, it provides a convenient tool to estimate the overall strength of flows in a street canyon. However, this model overestimates the velocity of street canyon flows at  $Re$  of order  $10^4$  [58]. Also, it is worth noting that the estimation is based on street canyons of height-to-width aspect ratio  $A = 1$ . In fact the three dimensionality of the street canyon flows depends not only on the height-to-width aspect ratio of a canyon, but also the length-to-height aspect ratio [71]. A lid-driven model is only valid for the skimming flow in a canyon with a large length-to-height aspect ratio where the ‘double-eddy circulation’ at canyon corners does not propagate into the centre of it. Thresholds of height-to-width and length-to-height aspect ratios for regime transitions were examined in detail in Ref. [71]. For long canyons with a length-to-height aspect ratio up to 7, the height-to-width ratios were determined to be 0.67 and 0.22 respectively for the transition from a skimming flow to an interference flow and further to an isolated roughness flow.

In addition to the strength of airflows, the size of the primary vortex is also an important feature of street canyon flows. For street canyons with a sufficient depth (large height-to-width aspect ratio), it was found in the lid-driven model given by Ref. [72] that the size of the primary vortex was proportional to  $Re^{1/2}$  for  $1500 < Re < 4000$ . It is also worth clarifying that the occurrence, size and position of the primary vortex for a cavity with a large aspect ratio at large  $Re$  beyond  $10^4$  are still not conclusive. One example is that Ref. [81] discovered multiple vortices of similar sizes in deep street canyons at  $Re = 1.5 \times 10^4$ , whereas Ref. [82] revealed only one primary vortex for the case with  $Re = 2.7 \times 10^6$ .

### 2.1.2. Shear-driven flow

A more realistic model of street canyon flows considers the shear flow on the roof, which can be referred as a shear-driven model. The presence of the shear flow on roofs has been noticed in many studies [56, 74,80]. A recent PIV measurement by Ref. [73] and a numerical simulation by Ref. [75] reveal the existence of such a shear layer, as shown in Fig. 4. Ref. [74] divided such a street canyon flow into four zones (i.e., Zones I, II, III and IV), refer to Fig. 2c. Zone II depicts a shear layer which separates the outer freestream flow (Zone I) and the inner cavity flow (Zone III). Zone IV represents the boundary layers at the walls.

It is expected that the flow in a street canyon is largely dominated by the shear flow at the roof. Depending on the strength of external turbulence, the mean velocity of the shear flow can be estimated by either Eq. (2) (low external turbulence) or Eq. (3) (high external turbulence) below:

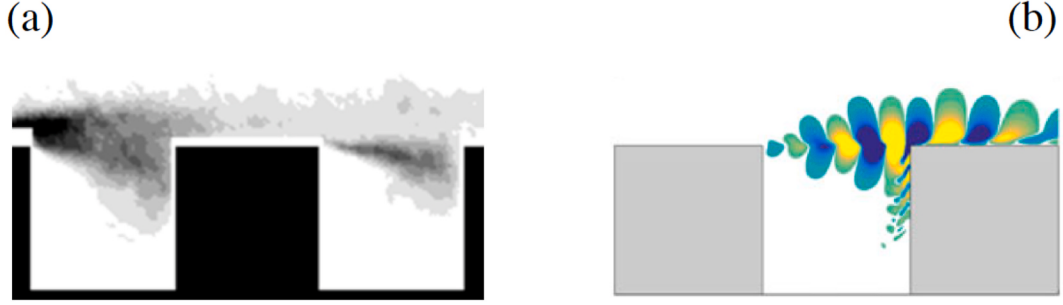


**Fig. 4.** (a) Sweep event in the shear layer estimated by  $-\langle u'v' \rangle / U^2$ , ranging from 0 to  $4 \times 10^{-3}$  [73], where  $u'$  and  $v'$  are the streamwise and vertical velocity fluctuation components,  $U$  the reference velocity at the cube height. (b) Vertical velocity fluctuations in the shear layer where yellow and blue colours denote positive and negative values [75].

$$\bar{U} = \frac{U_0}{2} \left( 1 + \text{Erf} \left( \frac{\sigma_0 Y}{X} \right) \right) , \quad (2)$$

$$\bar{U} = \frac{U_0}{2} \left( 1 + \text{Erf} \left( \frac{\sigma_h Y}{\sqrt{X}} \right) \right) , \quad (3)$$

in which  $\sigma_0 = 11$  and  $\sigma_h = \sqrt{U_0/4v_T}$  are nondimensional parameters for low and high turbulence scenarios [80].  $\sigma_0 = 11$  is an empirical value determined by experiments on jet flows [83].  $X$  and  $Y$  are the coordinates in the 2D canyon width and height directions respectively, and the origin is located at the upwind corner;  $U_0$  is the external velocity and  $v_T$  is the velocity fluctuation in the  $Y = 0$  plane. The importance of such correlations is that they can be combined with Eq. (1), in which the velocity of a moving lid represents the shear layer velocity.

#### (ii) Scales of circulation velocity

One of the most important characteristics of street canyon flows is the presence of a dominant standing vortex. The velocity of the circulation significantly affects pedestrian comfort, pollutant dispersion and heat removal. A scale of the circulation velocity can be estimated through a continuity equation [37]:

$$\beta V_c / H \sim U_c / W \sim U_\infty / W , \quad (4)$$

where  $U_c$  and  $V_c$  are the circulation velocity components in horizontal and vertical directions,  $U_\infty$  is the characteristic background velocity and  $\beta \approx 1$  for both inertially and thermally driven flows [37].

The correlation suggests that the horizontal velocity in the canyon is proportional to the freestream velocity, whereas the vertical velocity is dependent on the aspect ratio of the canyon. Ref. [84] found that the ratio of the circulation velocity at street to the wind velocity outside the street canyon is about 2/3. If the freestream velocity is sufficiently small, the standing vortex could be driven by buoyancy effect, which will be discussed in section 3.

#### (iii) Velocity approximations for various aspect ratios

The effects of aspect ratio on street canyon flows are complex [40,60,63], which have rarely been studied from the perspectives of mathematical modelling or scaling analysis. One of few analyses based on Operation Street Pollution Model (OSPM) pointed out a critical aspect ratio of 0.5 [74]. For a street canyon of  $H/W > 0.5$ , there are three flow regions as shown in Fig. 5a. Region I is outside the canyon and region III is adjacent to the ground. Due to the presence of the windward and leeward walls, region II is more influenced by the walls. For  $H/W < 0.5$ , two flow regions usually take place, as shown in Fig. 5 (b). The velocity profile at the centre of a narrow canyon ( $H/W > 0.5$ ) can be approximated by the logarithmic law in regions I and III, while region II can be described by an exponential growth function [86]. For wide street canyons, the influence of the vertical walls becomes less significant. Fig. 5 (c) shows the evolution of the velocity profile with changing aspect ratio. Multi-equation correlations for estimating the velocity profiles can be found in Ref. [74]. It is worth noting that the correlations given in Ref. [74] predict well the vertical profile of horizontal velocity in the upper part of the canyon (refer to the last two plots of Fig. 5a), but not the reverse flow of the standing vortex.

#### 2.1.3. Sectional remarks

Theoretical analyses and those models available to the community make it possible to understand and predict primary characteristics of street canyon flows without the demanding effort of numerical computation and field measurements. While the simplified lid-driven model has been accepted to be capable of capturing time-averaged velocity profile, the more realistic shear-driven model is able to distinguish different flow regimes within the simplified street canyon. This additional capacity of the shear-driven model can be of great importance to studies concerning spatial characteristics of street canyon flows, such as pollutant dispersion and removal from street canyons.

On the other hand, how to take coherent flow structures, side inflows and highly turbulent shear flow into account in theoretical modelling

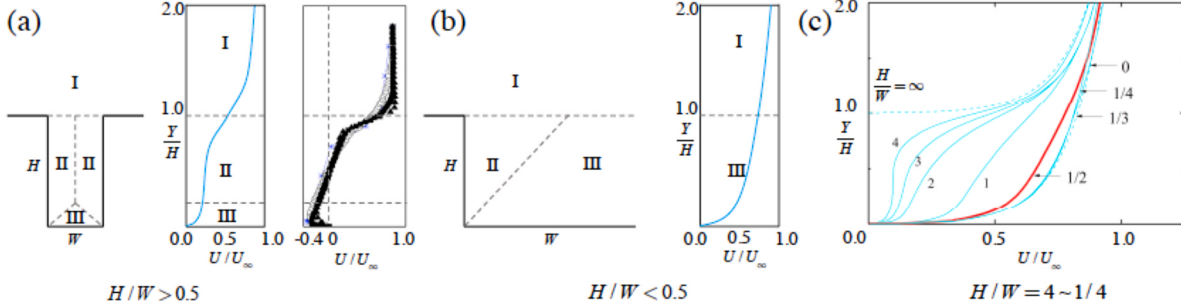


**Fig. 5.** Velocity profiles of the flow at the centre of (a) a narrow or (b) a wide street canyon from an Operation Street Pollution Model. (c) Velocity profiles indicating the influence of the aspect ratio [74]. The experimental data (markers) in the last plot of (a) are collected from Refs. [36,55,63,85]

are still open questions to the field. The leap from the modelling of simplified classical two-dimensional cavity flows to three-dimensional modelling considering side inflows is much needed since they play an important role in most of full-scale street canyon flows. Other challenging aspects for modelling flows in a realistic street canyon include the need to consider building density around the canyon of interest, local flow dynamics due to abrupt change of building geometries (e.g., step-up or step-down buildings), different building forms (e.g., different roof shapes, balconies, window sills, etc) and the presence of vegetation and even vehicles.

## 2.2. Experimental studies

One of the pioneering experimental studies on idealised cavity flows was performed by Ref. [72] by means of a photographic technique. A primary vortex was observed, and the study also pointed out that in the limit  $Re \sim \infty$  the primary vortex will remain, where the  $Re$  was determined by the velocity of the moving lid, the width of the cavity and the kinematic viscosity of the fluid.

Thanks to the emerging of the particle image velocimetry (PIV) technique, recent experimental studies have focused on the more realistic shear-driven cavity flows. Fig. 6a shows the flow structures observed by PIV measurements, which comprise a primary vortex within the cavity and vortices in the shear layer. Understandings and findings in regard to shear layer and flow dynamics within the cavity are reviewed and summarised below. A discussion on flow similarity between reduced-scale experiments and full-scale flows is given in section 3, where both isothermal and non-isothermal flows are covered.

### 2.2.1. Separated shear layer

The separated shear layer plays a vital role in the dynamics of flows within the street canyon, which has been examined experimentally in details by Ref. [76] and later by Refs. [80,57,87–89]. At low to moderate wind speeds, the formation of a shear layer at the upper part of a street canyon could even adversely affect the ventilation from the canyon to the outside of it [57]. It is now understood that subsequent small-scale vortices and the cluster of large-scale vortical structures are the consequence of the inflow turbulent boundary layer and the vortex-corner impingement.

It is seen in Fig. 6 (b) that vortices appear before the separation at the corner of the cavity, suggesting that the vortices at downstream positions are inherent structures of the inflow turbulent boundary layer. The formation of the cluster of large-scale vortices is more complex. It involves the interactions with the hairpin structures, the vortex-corner impingement and the cavity-wide recirculation vortex, as suggested by Fig. 6 (b). The mechanism of the vortex-corner interaction was documented by Ref. [90].

Quadrant analysis of shear stresses further reveals that sweeps (entrainment, denoted using  $Q_4$ ) and ejections (flushing, denoted using  $Q_2$ ) are the most dominant events in the shear flow that enters the upper part of a cavity [91]. The sweeps and ejections evolve spatially,

contributing to varied amount of turbulent kinetic energy in different regions of the cavity [73,92]. Fig. 7 shows an alternating occurrence of sweeps and ejections. Recent wind tunnel measurements also reveal that these two events affect the transport of scalars in the cavity significantly [46,89].

### 2.2.2. Structure of flow within cavity

The flow structure within the cavity is dominated by the shear layer flow along the cavity and the geometrical properties of the cavity. The shear flow alternates sweep and ejection events where vortices shed from the corner of the leeward wall propagate downstream. The train of vortices subsequently impinges the corner of the windward wall and separates into two streams. One of them penetrates into the cavity along the trailing (windward) wall. This stream of flow then turns and travels along the bottom and leeward walls of the cavity. The large-scale cavity-wide circulation flow is enclosed by those boundary layer-like flows along the walls of the cavity. Such a dynamic physical mechanism was clearly revealed by PIV measurements [76].

The effects of the shear layer on the flow within the cavity is characterised by either the  $Re$  defined with cavity height [56,57,89,93] or the  $Re_{mt}$  estimated using the scale of the shear layer momentum thickness [76,94,95]. For unit-ratio street canyon flows, the PIV results by Ref. [56] suggest that the critical Reynolds number is around  $10^4$ , beyond which only one primary vortex is observed. The Reynolds number based on momentum thickness was found to be  $Re_{mt} = 830$  for a bulk Reynolds number at 11,650 for a unit-ratio street canyon flow [87].

For street canyon flows with large aspect ratios ( $H/W > 1.5$ ), the critical Reynolds number is found to increase with the aspect ratio. For instance, the critical Reynolds number is found to be between 57,000 and 87,000 for street canyon with an aspect ratio of 2.0 [93]. Shallow street canyon flows were experimentally examined in Refs. [94,95]. Ref. [94] found that the characteristics of the shear layer depend on the in-canyon coherent vortical structures. Ref. [95] revealed that for a shallow street canyon with  $H/W = 0.25$ , the oscillation of flow structures within the cavity is due to the build-up of the flow, rather than the vortex shedding from the shear layer on the top of the cavity.

Experimental studies also examined the effects of roof geometry on flow dynamics within a street canyon [57,96]. Ref. [96] reported that flat roofs produce less turbulent flow whereas pitched roofs induce flows with larger vortices penetrating into the street canyon. The ventilation in the upper part of the canyon was found to be strengthened by the pitched roofs. Step-up and step-down buildings were also studied [57]. The presence of three-dimensional flow structures induced by non-uniform building height was thought to be a key factor affecting ventilation in street canyons, although flows in street canyons with non-uniform building height are mostly simplified to two-dimensional flows in experimental studies. Also, from the same perspective, the ‘breathability’ of lined up street canyons which suggests the removal capacity of scalars, was quantified by water tunnel PIV measurements with the mean exchange velocity between the flow within the street canyon and at the urban canopy level [102]. A reduction of more than

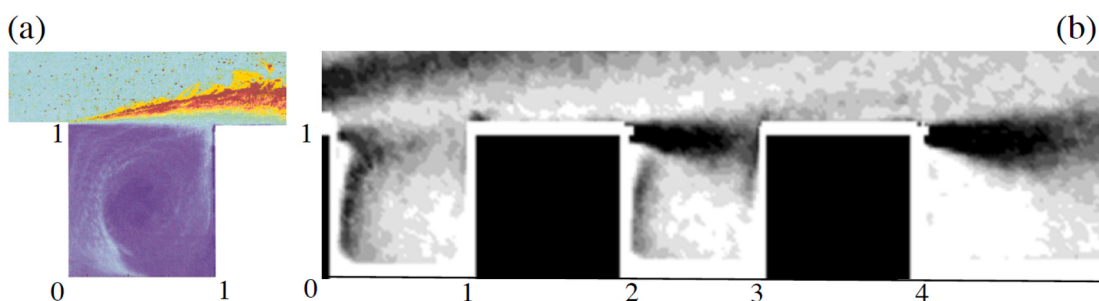


**Fig. 6.** (a) The shear layer and large-scale in-cavity vortex depicted by relative RMS fluctuations of concentration fields ranging from 0 to 3 [80] and (b) conditional averaging of mean spanwise vorticity ranging from 0 to 0.05 [73].

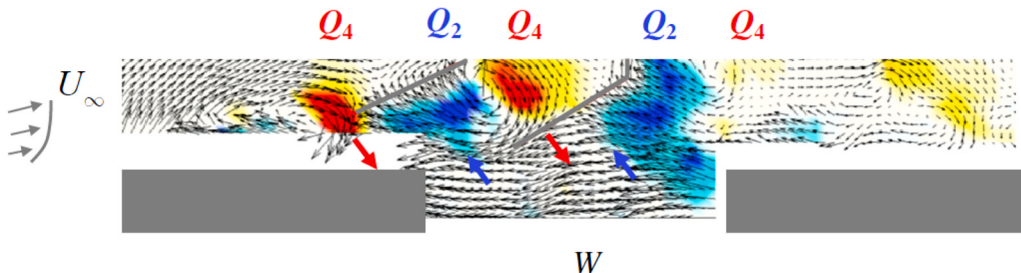


**Fig. 7.** A quadrant analysis showing alternating ejection ( $Q_2$ ) and sweep ( $Q_4$ ) events in the shear layer. The contours show  $-0.1 < Q_2 < 0$  and  $0 < Q_4 < 0.1$  where fluctuating velocity components are normalised using  $U_\infty$  [73] and the solid grey lines indicate stagnation regions. Note that the experiment was performed with cubes placed apart at a distance equal to the cube width. This figure only shows the upper part of the cubes.

50% of breathability capacity was noted as the density of two-dimensional street canyon models was doubled to be 0.67. Ref. [108] measured pollutant concentrations in a street canyon with

non-porous and porous tree models and found overall greater concentration compared to a street canyon without trees.

Some representative experimental studies are summarised in

**Table 1**  
Experimental studies on isothermal street canyon flows.

References	Config. <sup>a</sup>	$Re$ or $Re_{mt}$ <sup>b</sup>	$A$ ( $H/W$ )	Exp. Approach <sup>c</sup>	Key words	Remarks
[72]	L-D, 2D	$O(10) \sim O(10^3)$	1/4–5	Photographic technique, (W)	Single and multiple vortices	d
[97]	S-D, 2D	$O(10^3)$	2/3–10/9	PIV, (W)	Landscape influence	e
[98]	S-D, 2D	$O(10^4)$	1–3	PIV, (F)	Multiple vortices	f
[76]	S-D, 2D	$O_{mt}(10^3)$	1/4–1	PIV, (W)	Impingement process	g
[80]	S-D, 2D	$O(10^4)$	1	PIV, (W)	Shear layer separation	h
[94]	S-D, 2D	$O(10^5)$	1/2, 1/3, 1/4	PIV, (W)	Three regions of shear layer	i
[99]	S-D, 2D	$O(10^4)$	1/2, 1, 2	LDV, (W)	Different flow regimes	j
[95]	S-D, 2D	$O_{mt}(10^3)$	1/4	PIV, (W)	Oscillation mode	k
[100]	S-D, 2D	$O(10^4)$	1, 2, 1/2	HWA, (W)	Two-scale roughness	l
[101]	S-D, 3D	$O(10^4)$	1	UA, (FM)	Atmospheric flow over cubes	m
[77]	S-D, 3D	$O_{mt}(10^3)$	1/4, 1/2, 1	PIV, (W)	Large-scale structures	n
[88]	S-D, 2D	$O(10^3) \sim O(10^4)$	1/2	PIV, LDV, (W)	Modal spatial structures	o
[96]	S-D, 2D	$O(10^4)$	1	PIV, (W)	Pitched roofs enhance ventilation	p
[56]	S-D, 2D	$O(10^4)$	1	PIV, (W)	Reynolds independent regime	q
[102]	S-D, 2D	$O(10^4)$	3/7–2	PIV, (F)	Mean exchange velocity	r
[103]	S-D, 3D	$O(10^4)$	3/2–15/4	PIV, (W)	Transition of flow regimes	s
[89]	S-D, 2D	$O(10^4)$	~1	PIV, (W)	Influence of incoming turbulence	t
[104]	S-D, 2D	$O(10^4)$	10/7	PIV, (W)+(FM)	Intermittency of flow structures	u
[105]	S-D, 2D	$O(10^4)$	1	Fog experiments, (W)	Influence of different roofs	v
[106]	S-D, Field	$O(10^5)$	~1	PIV, (F)	Varied background wind	w
[46]	S-D, 3D	$O(10^4)$	1/15–1	HWA, (W)	Role of intermittent motion scales	x
[107]	S-D, 3D	$O(10^4)$	N.A.	PIV, (W)	Isolated roof and its effects	y

<sup>a</sup> L-D refers to lid-driven; S-D refers to shear-layer driven; 2D refers to 2D canyons without side inflow; 3D refers to 3D canyons with side inflow.

<sup>b</sup>  $Re$ : defined based on the scale of the cavity height; its order of magnitude is denoted by  $O( )$ .  $Re_{mt}$ : defined based on the scale of the momentum thickness of the incoming shear layer; its order of magnitude is denoted by  $O_{mt}( )$ .

<sup>c</sup> PIV refers to particle image velocimetry, HWA the hot wire anemometry, LDA the laser doppler anemometer and UA the ultrasonic anemometer. (W) Refers to wind tunnel, (F) the water flume (tunnel) and (FM) the field measurements.

<sup>d</sup> Flow patterns were determined experimentally, and multiple vortices were observed for deep cavities.

<sup>e</sup> The profile of upstream landscape was found to strongly affect the pollutant dispersion within the canyon.

<sup>f</sup> Two counterrotating vortices were observed in a step-down canyon.

<sup>g</sup> The impingement progress and the subsequent separation of wall-jet like shear flow were revealed.

<sup>h</sup> The shear layer dominates the transfer between the external flow and the street canyon.

<sup>i</sup> There are three regions of a shear layer separated from the leading edge of a cavity.

<sup>j</sup> A low frequency oscillation model was found and distinguished from the vortex shedding of the shear layer.

<sup>k</sup> The aspect ratio of 0.5 resulted in the wake interference flow regime at the Reynolds number examined.

<sup>l</sup> Small-scale roughness on building roofs was found to increase the turbulence intensities and momentum transfer of the flow.

<sup>m</sup> Inner-layer scaling similarity was found in the turbulent atmospheric flow over an array of cubes.

<sup>n</sup> Large-scale vortical structures were detected, which were believed to be responsible for the self-sustained oscillation modes.

<sup>o</sup> Two different shear layer modes were revealed.

<sup>p</sup> Pitched roofs results in more disturbed flow in the upper part of a canyon.

<sup>q</sup> For street canyon flow at aspect ratio of 1 the Reynolds number independent regime is above 13,000.

<sup>r</sup> The street canyon flows are studied from the perspective of flow exchange processes and breathability.

<sup>s</sup> Increasing the height of a downstream building resulted in the flow regime transition from wake dominated to wake interference regime.

<sup>t</sup> Three different mechanisms for the production of coherent structures were discussed.

<sup>u</sup> The intermittency of the main vortex structure was demonstrated.

<sup>v</sup> Pitched and round roofs influenced the in-canyon mean and turbulent velocities.

<sup>w</sup> The heterogeneity and natural variability of background wind were studied using water tunnel PIV and PLIF measurements.

<sup>x</sup> Rougher urban surfaces promote street-level ventilation.

<sup>y</sup> Roof shapes were found to affect the wind conditions at the pedestrian level.

**Table 1.** Key characteristics of those studies and their findings are also concluded. It is worth noting that the summary here only concludes the findings that are in close relevance to the scope of this review.

### 2.2.3. Sectional remarks

Extensive understanding of street canyon flows and their main behaviour, such as the canyon-wide standing vortex, the events of sweep and ejection, the shear layer and associated vortex shedding, the effects of street canyon aspect ratio and geometrical features of buildings, has been documented to a great extent. These experimental studies have been mainly devoted to two-dimensional, time-averaged and simplified street canyon models with wind tunnel measurements using particle image velocimetry.

The presence of small-scale roughness on building roofs has been found to promote ventilation and scalar dispersion at street-level. In realistic street canyons, building surfaces and ground are often constructed using porous façade materials and pavements in different form articulation. The influence of these engineered materials and architectural forms (e.g., roof overhang, window sills, balconies, etc) on large scale street canyon flows and turbulence intensity is rarely measured.

To further enhance the understanding of street canyon flows, future works are desired aiming:

- to perform time-resolved three-dimensional (e.g., stereo- and tomographic-PIV) measurements which will provide essential data for development and validation of turbulence models;
- to implement measurements with time-dependent wind direction which has been predominantly assumed to be either perpendicular or oblique to the street canyon of interest;
- to study the influence of material articulations and forms at various scales on street canyon mean flow, turbulence intensity and resultant pollutant dispersion;
- to extend experimental studies to street canyon flows in the context of neighbourhood where an inhomogeneous spatial profile of buildings has a vital role; and
- to complement field measurements within street canyons and up to the urban canopy layer which are of paramount importance to the development of urban parametrization models.

### 2.3. Numerical simulations

In comparison to wind-tunnel measurements, including the build-up of the experimental setup and acquisition of specialised measurement equipment, the use of numerical simulations for flow analysis is typically less time consuming and less expensive. Furthermore, numerical simulations can provide detailed flow information, both spatial and temporal, at every location of the computational domain. While these advantages are some of the reasons for the increasing number of numerical studies [109], they require model validation in order to use with confidence.

Appropriate boundary conditions are the key to successful CFD model validation. As outlined by the guidelines in section 2.3.1, at the outlet, a “free” boundary condition is preferentially prescribed, where the normal gradients of all variables are set to zero. At the lateral and top boundaries, free-slip or symmetry boundary conditions are prescribed. At the inlet, a velocity profile and the relevant turbulence quantities are specified as boundary conditions. This is a straightforward approach for model validation using wind tunnel tests, since the far upwind velocity and turbulence profiles can be measured and prescribed at the inlet of the CFD model. The inlet and outlet boundaries can also be dealt with blending zones for building-resolved nested-LES [110]. The introduction of blending zones enables smooth transition of turbulent structures at inflow and outflow boundaries.

For model validation with field measurements, upwind meteorological measurements often have low spatial resolution and interpolation is needed to determine the most appropriate boundary conditions at

the inlet of the CFD model. This highlights a major difference of model validation between reduced-scale experiments and full-scale field measurements. In addition to the domain boundary conditions, different boundary conditions on building surfaces have to be specified. In reduced-scale experiments, “buildings” are represented with idealised geometries with smooth surfaces, whereas real, full-scale buildings can have complex geometries with rough surfaces. Therefore, care must be taken while prescribing the building boundary conditions, for example, whether a smooth or rough wall function should be used. Similarly, for the ground, roughness elements (such as vegetation and small urban structures that are not modelled explicitly) need to be considered in model validation involving realistic built environment. Lastly, we emphasize that a CFD model validated at reduced scale may not accurately predict the flows at full scale. This will be discussed in Section 2.3.4.

#### 2.3.1. Guidelines and recommendations

High quality reviews of street canyon flow modelling using computational fluid dynamics (CFD) are available in the literature [111–114]. We will not repeat them but briefly outline the methodology with emphasis on recent advances. Ref. [115] summarised the steps in CFD modelling with two example case studies. Best practice guidelines for CFD modelling are also available in the literature [111–114]. Note that these guidelines are not specific to flows in street canyons. Nevertheless, many CFD studies focus on street canyons as a generic element in the urban environment. Reviews of various turbulence models and roughness height are also available in Refs. [116,117].

Despite these guidelines highlighting the importance of model validation, the recent review by Ref. [109] revealed that among the 183 reviewed studies, 105 were conducted without validation. They suggested that when researchers cannot produce their own experimental data for validation, they should use measurement data available online. Requirements for validation data based on field and wind-tunnel measurements are provided by Refs. [118,119]. Some available resources for validation and modelling purposes are listed below:

- The CEDVAL database of the University of Hamburg (<https://mi-pu.b.cen.uni-hamburg.de/index.php?id=433>).
- The CODASC database of the Karlsruhe Institute of Technology (<http://www.ifh.uni-karlsruhe.de/science/aerodyn/CODASC.htm>).
- The database by the Architectural Institute of Japan ([http://www.aij.or.jp/jpn/publish/cfdguide/index\\_e.htm](http://www.aij.or.jp/jpn/publish/cfdguide/index_e.htm)).
- Urban climate modelling at street canyon scale, Chair of Building Physics at ETH Zürich (<https://carmeliet.ethz.ch/research/urban-microclimate.html>).

#### 2.3.2. Numerical modelling of turbulence

The guidelines mainly aim to limit errors in CFD analyses, which can be divided into two broad categories [120]: 1) physical modelling errors related to uncertainties in the formulation of the problem and to deliberate simplifications in the model, e.g., due to the choice of turbulence model, use of wall functions, simplifications in geometrical complexity and physical boundary conditions, 2) numerical errors related to the numerical solution of the model, e.g., due to convergence criteria and discretization schemes.

Reynolds-averaged Navier–Stokes (RANS) and large eddy simulation (LES) are the most commonly-used turbulence modelling approaches for CFD analyses. Comparisons between RANS and LES [58,121–124] show that LES models are often more accurate than RANS models. Nevertheless, RANS models are much more commonly adopted in street canyon flow modelling due to their relatively low computational cost. RANS-based studies mostly use steady analysis, as opposed to unsteady RANS (URANS), even though the atmospheric boundary layer is inherently unsteady. Guidelines in general recommend the use of hybrid URANS/LES or LES models instead of URANS due to their higher accuracy [112]. Despite the dramatic increase of computational power in

the 2000s, LES has not replaced RANS [125], as fewer than 4% of 176 studies between 1998 and 2015 reviewed by Ref. [109] adopted LES. In addition to the higher computational cost of LES, the lack of best practice guidelines for LES models could also make RANS the more common choice [114,126]. Therefore, developing a comprehensive guideline for LES evaluations could help to advance the use of LES in modelling of street canyon flows. LES further requires time and space resolved inflow boundary conditions, which can be difficult to obtain [112]. Examples of hybrid URANS/LES studies are also relatively scarce [114].

While the adoption of LES is slow in modelling of street canyon flow, reduced order modelling (ROM) [127] has gained attention due to its capability for real-time prediction [128]. The concept of ROM is not new (e.g., applications in fluid mechanics in the 1990s [129,130]), but its applications in built environment has not become popular until recently. Ref. [131] simulated pollutant dispersion in 2D and 3D street canyons using LES and ROM. Compared to the LES results, ROM captures both the flow fields and tracer profiles accurately, with up to 98% reduction in computational time. Ref. [132] simulated pollutant dispersion from a nuclear power plant using RANS and ROM. They reported that the results are comparable, with ROM achieving a  $10^5$  reduction in computational power. Refs. [133,134] demonstrated ROM's ability to accurately predict the flows in both 2D and 3D street canyons and real built environments with a case study in the London South Bank University campus. Compared to LES, ROM can predict the mean flow field accurately with less computational power, but not the Reynolds stresses. The performance of ROM can be improved by increasing the number of reduced basis functions at higher computational cost, but the cost is still significantly lower (by six orders of magnitude) than that of LES. With the enormous reduction in computational resources needed in ROM compared to full CFD models, it will be possible to achieve real-time simulations of urban airflows using ROM in the near future.

### 2.3.3. Geometrical modelling

The isothermal lid-driven cavity flow is a classical problem with numerical studies dated back to the 1960s [72,135]. Today, the isothermal lid-driven cavity flow can be modelled with the simplest numerical model and is often used as the first test of validation, for example in the open-source software OpenFOAM [136]. Flows across street canyons are more complex than the lid-driven cavity flows. Fortunately, the abundance of wind tunnel measurements on street canyon flows enables validation of numerical simulations of these flows. These measurements are not without limitation: they are often conducted with idealised building geometry. However, it is common to use measurements of idealised geometry to first validate a CFD model (of idealised geometry), then use the same CFD model in studies involving more complex geometry. For instance, experimental data of idealised street canyons with flat roofs was used to validate CFD models (with flat roofs) and subsequently, the CFD models were extended to study street canyons with pointed roofs [137,138]. Another example is the studies of building porosity, where experimental data of idealised street canyons (without porosity) was used to validate the CFD models and subsequently, the CFD models were extended to study street canyons with building porosity [34,139].

### 2.3.4. Validation with reduced-scale experiments

From the above discussion, it is common and seemingly accepted in the community to adopt the strategy in practice. Although this is convenient, we can achieve higher confidence in the accuracy of CFD models by taking a step further to validate the CFD models with experimental data having a similar configuration or sub-configuration [114]. For instance, CFD models simulating pointed roof can be validated with experiments of pointed roof instead of flat roof [140], and CFD models simulating building porosity can be validated with experiments of models with porosity instead of idealised models [31,141].

CFD models are often validated with reduced-scale experiments. The Reynolds-number independence criterion then allows these CFD models

to perform full-scale studies by assuming that flows at full scale behave similarly as flows at reduced scale when a sufficiently high Reynolds number is achieved. The Reynolds number independence criterion provides a very convenient circumvention of the mismatch of dimensionless parameter, to the extent that it has been “abused” [142]. The Reynolds numbers based on building height and atmospheric wind speed are in the orders of  $10^5$ - $10^7$ . In reduced-scale experiments, while it is easy to maintain wind speeds similar to those in a real atmosphere, building models are scaled down by two or even three orders, thereby reducing the Reynolds number by two to three orders of magnitude. The flow dynamics can vary across such a large decrease of Reynolds number, and thus measurements at reduced scale may not reproduce the expected flow dynamics at full scale. Furthermore, the Reynolds number required to achieve Reynolds number independence is case-specific (e.g., canyon aspect ratio) and region-specific (e.g., distance from the canyon wall) [143]. For instance, reduced-scale experiments reveal that narrow street canyons (with aspect ratio  $\geq 2.0$ ) induce two vortices in the canyons [98,99]. CFD models predict this double-vortex flow field correctly at reduced scale [62,144] and are thus considered validated. These “validated” models are then used to simulate full-scale canyons, or the results were generalised to full-scale applications. However, full-scale measurements show that only one primary vortex is induced in narrow street canyons [82], invalidating CFD models “validated” at reduced scale showing two vortices. In fact, CFD simulations at high Reynolds number ( $Re > 10^5$ ) reveal only one vortex in narrow street canyons [145–148], consistent with the field measurements. When full-scale measurements are not available for model validation, CFD simulations validated with reduced-scale experiments should be repeated at higher Reynolds numbers to verify that Reynolds number independence is achieved, for example in Refs. [145,149].

Simulations at full scale mostly make use of wall functions for wall treatment, as resolving viscous sublayer is computationally too demanding. Wall functions require the near-wall cell centre to be located in the fully-turbulent log-law region, i.e., between 30 and 500 in terms of the nondimensional wall distance  $y^+$  [112]. However, this requirement typically does not hold in full-scale simulations of atmospheric boundary layer (ABL) flows, which can be considered as a limitation that creates uncertainty in results. Furthermore, in cases with rough wall functions, high  $y^+$  values are a direct result of the requirements of roughness modifications [150]. Ref. [151] stated that there is a need for an alternative definition of  $y^+$  when rough walls are used. Nevertheless, validation studies showing good agreement with field measurements have been performed using wall functions with  $y^+$  values larger than the required range [152,153]. It is also often argued that the effect of wall functions on the flow field far away from the wall is limited [112]. However, deficiencies related to wall treatment can be more critical in cases such as heat transfer, which is further discussed in section 3.3.

### 2.3.5. Sectional remarks

Overall, despite its limitations, CFD is particularly convenient when large number of cases under controlled conditions, e.g., parametric studies, are compared based on different scenarios. Keeping advantages of CFD in mind with validation requirements, numerical and experimental methods should be considered complementary to each other with different level of insight and accuracy [154,155]. Despite its capacity to model full-scale built environment, many CFD studies of street canyon flows are/were still performed at reduced-scale, mainly because the models are/were validated with reduced-scale experiments. Due to its high computational cost, the more accurate LES is less commonly adopted than RANS. Some suggestions to close these research gaps in numerical modelling include:

- more robust model validation, ideally with full-scale measurements;
- computationally-efficient models with acceptable accuracy in the context of a study; and

- fast models that can perform real-time simulations and predictions.

### 3. Advances on non-isothermal flows

#### 3.1. Theoretical analyses

##### 3.1.1. Relaxed similarity

Street canyon flows are mostly studied by reduced-scale experiments and numerical simulations. The starting point of these studies is always the similarity analysis, where the unique nondimensional numbers characterising the flow under consideration should be matched between the full-scale and reduced-scale flows.

However, except for studies involving full-scale field measurements, similarity of nondimensional numbers cannot be fully satisfied for most reduced-scale experiments. To facilitate discussion, the momentum, continuity and energy equations are given below in nondimensional forms [156]:

$$\frac{\partial U_i^*}{\partial t} + U_j^* \frac{\partial U_i^*}{\partial x_j} + \frac{2}{Ro} \varepsilon_{ijk} U_k^* \Omega_j^* = -\frac{1}{\rho} \frac{\partial \delta P^*}{\partial x_i^*} + \frac{1}{Fr^2} \delta T^* \delta_{3i} + \frac{1}{Re} \frac{\partial^2 U_i^*}{\partial x_j^* \partial x_i^*}, \quad (5)$$

$$\frac{\partial U_i^*}{\partial x_i^*} = 0, \quad (6)$$

$$\frac{\partial \delta T^*}{\partial t} + U_i^* \frac{\partial \delta T^*}{\partial x_i^*} = \frac{1}{Pe} \frac{\partial^2 \delta T^*}{\partial x_i^* \partial x_i^*}, \quad (7)$$

where  $Ro = U_\infty / L \Omega_R$  is the Rossby number,  $Fr = U_\infty / (gL \delta T_R / T_0)^{1/2}$  the Froude number,  $Re = U_\infty L / \nu$  the Reynolds number and  $Pe = U_\infty L / \kappa = Re \cdot Pr$  the Peclet number.  $Pr$  is the Prandtl number.  $L$  is a length scale,  $\Omega_R$  the angular velocity,  $U_\infty$  the reference velocity and  $g$  the gravity.  $\delta T_R$  and  $T_0$  are the temperature deviation due to height variation and the temperature of a neutral atmosphere (height dependent), respectively. Fluid properties are the density  $\rho$ , the kinematic viscosity  $\nu$  and the thermal diffusivity  $\kappa$ .  $\varepsilon_{ijk}$  is the alternating tensor and  $\delta_{ij}$  Kronecker's delta. The prime denotes dimensionless quantity.

To achieve rigorous similarity between full-scale and reduced-scale flows, the four characteristic numbers should be identical at both scales, along with identical nondimensional boundary conditions. By taking the scaling factors in the orders of 10, 100 and 1000, and considering the physical properties of commonly used fluid media (air and water) it is immediately clear that for scale-ratios in the order of 100 and above, rigorous similarity cannot be achieved for all characteristic numbers.

A first relaxation can be easily made by dropping the similarity of  $Ro$  for studies at street canyon scale well within the most conservative criterion of 5 km [156]. The second relaxation is the  $Pe$  similarity, especially for studies using water as a fluid media. When the  $Re$  similarity is satisfied for water tunnel experiments, the mismatch in  $Pe$  is inevitable. Therefore, the similarity of  $Pe$  has to be relaxed for water tunnel experiments. On the other hand, the  $Pe$  similarity can be approximately met if using air as fluid medium since the  $Pr$  does not change much from full-scale to reduced-scale flow.

For flows in which thermal effects come into play, the similarity of  $Fr$  also needs to be satisfied. However, the similarity of  $Re$  and  $Fr$  cannot be satisfied at the same time for a scale-factor on a typical order of 100 or above. An acceptable treatment in physical and numerical modelling is to relax  $Re$  by pushing the flow under consideration into a  $Re$  independent regime. As to the similarity of  $Pe$  in non-isothermal flows, the similarity of  $Pe$  has to be relaxed in water measurements whereas it is approximately met if air is used in modelling.

The similarity and relaxation of characteristic numbers for common wind tunnel and water tunnel studies are summarised in Table 2, where '✓' indicates full satisfaction, '~~' approximate satisfaction and 'Rela.' relaxation. It is worth noting that full satisfaction of  $Re$  in wind tunnel studies can only be achieved when the  $Re$  is relatively small, for instance

**Table 2**

Similarity and relation of characteristic numbers for modelling of isothermal and non-isothermal street canyon flows. '✓' indicates full satisfaction, '~~' approximate satisfaction and 'Rela.' Relaxation.

Characteristic number	Isothermal		Non-isothermal		
	Re	Pe	Re	Fr	Pe
Wind tunnel measurements	✓/Rela.	~~	Rela.	✓	~~
Water tunnel measurements	✓/Rela.	Rela.	Rela.	✓	Rela.

in the order of  $10^3$ - $10^5$ . It is also worth clarifying that the  $Re$  independence is geometrically sensitive, as pointed out in Ref. [156]; and more recently in Ref. [93]. A very recent study in Ref. [143] further revealed that the  $Re$  independence of isothermal street canyon flow is flow-region dependent. In the canyon and above building roofs, the critical  $Re$  is determined to be  $1 \times 10^4$  -  $3 \times 10^4$ , while for near-wall region the critical  $Re$  is  $6 \times 10^4$  -  $1.4 \times 10^5$ . On non-isothermal street canyon flows, a critical  $Re$  is approximately determined to be  $3 \times 10^4$  for the flow probed at the centre of canyons [56]. It is expected that critical Reynolds numbers for non-isothermal street canyon flows in near-wall and near-ground pedestrian regions may differ, which deserve future explorations.

In the case one or more characteristic numbers have to be met approximately or even relaxed, particular cautions need to be paid to the validity and accuracy of full-scale and reduced-scale studies. The validity and accuracy mainly depend on whether the studies are performed in the  $Re$  independence regime. However, such a  $Re$  independence regime depends not only on geometrical similarity, but also on the aerodynamic similarity. Existing understanding of the latter is still limited, which may lead to inappropriate validation.

##### 3.1.2. Gradient and bulk richardson numbers

In atmospheric science two commonly used variants of Richardson number are the gradient and bulk Richardson numbers. The gradient Richardson number is mainly adopted to characterise the instability between buoyancy and gravitational acceleration. A typical form of the gradient Richardson number is given as [157]:

$$Ri = \frac{g}{T_v} \frac{\partial \theta_v / \partial z}{(\partial U / \partial z)^2 + (\partial V / \partial z)^2}, \quad (8)$$

where  $g$  is the gravity,  $T_v$  the absolute virtual temperature,  $\theta_v$  the virtual potential temperature,  $z$  the depth of the layer,  $U$  and  $V$  the horizontal wind components.

It is worth noting that the gradient Richardson number is mostly used to assess local instability of a thin atmospheric layer. A critical value of 0.25 is commonly accepted [158], which applies for local gradients. On the other hand, the bulk Richardson number (see equation (9)) is widely adopted to characterise the ratio between buoyant convection and shear flow of a finite fluid layer. In meteorology, the bulk Richardson number is an approximation of the gradient Richardson number.

A more realistic model of street canyon flow, especially under conditions of low wind speed, considers the influence of buoyant flows induced by heated façades and ground surfaces due to absorption of solar radiation. The pioneering study on non-isothermal street canyon flows by Ref. [84] essentially used the bulk Richardson number in the form:

$$Ri = \left( g / \bar{T} \right) \left( \Delta \bar{T} / \Delta Y \right) \left( \Delta \bar{U} / \Delta Y \right)^{-2}, \quad (9)$$

where  $g$  is the gravitational acceleration,  $\bar{T}$  the mean canyon temperature,  $\Delta \bar{T} / \Delta Y$  the mean vertical difference of air temperature and  $\Delta \bar{U} / \Delta Y$  the mean vertical difference of the horizontal wind speed in the canyon. The quantities here are dimensional.

By substituting  $\Delta Y$  with the cavity height  $H$ , the above correlation can be rewritten as below,

$$Ri = \left( gH\Delta\bar{T}/\bar{T} \right) / \left( \Delta\bar{U} \right)^2 , \quad (10)$$

which is the typical form of bulk Richardson number that is widely used in the field. The term  $\Delta\bar{T}$  here characterises the difference of average temperature over the height of the canyon and  $\Delta U$  represents the difference of horizontal velocity components at the roof and the ground.

In recent studies,  $\Delta\bar{T}$  is usually characterised using a bulk (average) temperature difference between the air at the roof/ground level [57,63], between windward/leeward walls [37,44] or between a known surface/ambient air [159]. The  $Ri$  estimated with those average temperature differences essentially characterises bulk fluid dynamics of the street canyon, which is also referred to as the bulk Richardson number. The critical bulk Richardson number that distinguishes whether a street canyon flow is dominated by buoyancy effects or incoming wind is 0.5–1.0 [69].

### 3.1.3. Scales of buoyant plume from heated building walls

Due to the absorption of solar radiation, surface temperature of building walls is usually higher than the surrounding air temperature, which results in a buoyancy-driven boundary layer flow adjacent to the wall, as illustrated in Fig. 8. Scaling analyses of this type of buoyancy-driven flows give important scales (analytical correlations) of various characteristics that are in direct relevance to understanding and modelling of street canyon flows.

As shown in Fig. 8, the boundary layer flow adjacent to a building wall comprises a laminar region, an intermediate-height region and a large-height region (distinguished by short dotted lines). The large-height region can be in the order of 100 m. The scaling analysis revealed that in those intermediate- and large-heights regions, the vertical velocity ( $V$ ), temperature ( $T_0$ ) and the width of the plume ( $W_p$ ) can be estimated in an average sense. These scales are read as [160]:

$$V = \left[ \frac{4\beta_1}{5E_2(1+\beta_1)(PrRa_c)^{1/3}} \right]^{1/3} (g'k)^{1/9} (g'Y)^{1/3} , \quad (11)$$

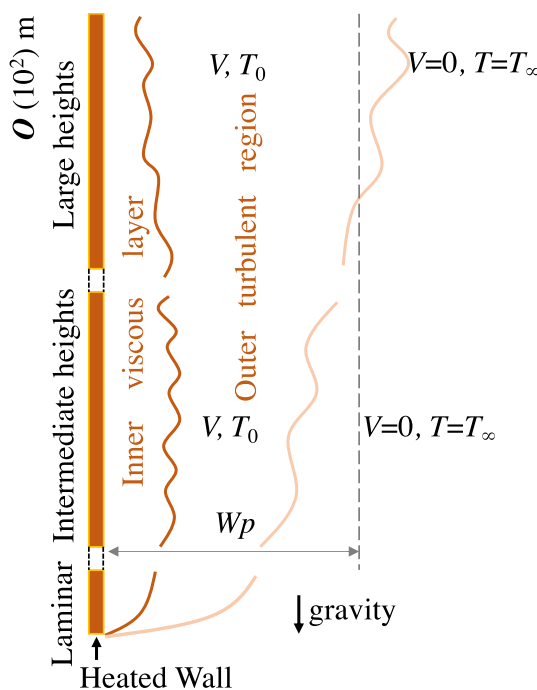


**Fig. 8.** Characteristics of buoyancy-driven plume from heated building walls [160].  $V$  is the vertical velocity,  $T$  the temperature and  $W_p$  the average width of the plume.

$$T_0 = \frac{5}{3Pr} \left[ \frac{4\beta_1 Pr}{5E_2(1+\beta_1)(PrRa_c)^{1/3}} \right]^{2/3} (T_w - T_\infty) \left[ \frac{v}{(g'k)^{1/3} Y} \right]^{1/3} + T_\infty , \quad (12)$$

$$W_p = \frac{3}{4} E_2 Y , \quad (13)$$

where the transport property  $\beta_1 = 0.34$ , the entrainment coefficient  $E_2 = 0.135$  and the height  $Y$  of a heated wall.  $g'$  is the reduced gravity,  $\kappa$  the ambient fluid density and  $T_w$  the surface temperature of the heated wall.  $Pr$  is the Prandtl number and  $Ra_c$  is the critical Rayleigh number. It is worth noting that these scales are valid for the boundary layer adjacent to a building of height up to 140 m. The importance of these scales is that the thickness and velocity of the buoyancy-driven plume can be estimated conveniently without complex simulations. The scales can also be used to predict if thermal effects need to be considered in numerical modelling, which will be further discussed in section 4.

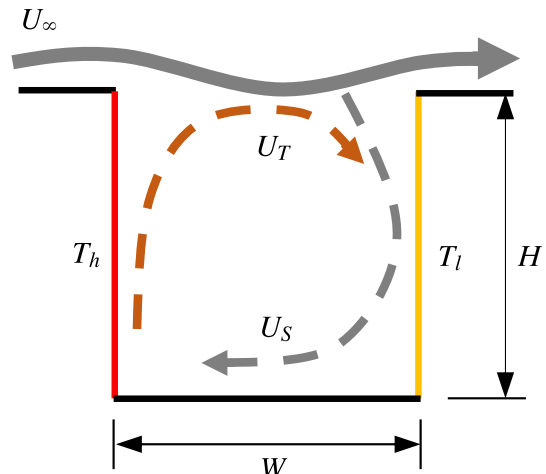
### 3.1.4. Scales for canyon-wide circulating flow

Fig. 9 gives an example of the canyon-wide circulation when the windward wall is at low and the leeward at high temperature (denoted by the red line). Due to the presence of the shear layer at the roof of a canyon, the upward thermal plume induced by the hot leeward wall cannot fully penetrate the shear layer and hence part of it continues to travel horizontally and later penetrates back into the canyon along the less heated windward wall. This process is recognised as a thermally-driven circulation, of which the horizontal velocity is  $U_T$ .

The circulation can also be driven by the separated shear flow in the case without thermal effects, which is the representative standing vortex and the horizontal velocity is  $U_S$ . When it comes to the scenario that both the thermal effect and the shear layer flow are considerable, a scale that distinguishes the dominant mechanism can be derived to be [37]:

$$B = \left[ \frac{ga(T_h - T_l)H}{U_\infty^2 [1 + (H/W)^2]} \right]^{1/2} \gg B_C , \quad (14)$$

where  $\alpha$  is the thermal expansion coefficient of air and  $B_C$  the critical characteristic number. A suggested value of  $B_C$  was given to be 0.05, which was supported by measurement from Refs. [37,56,161]. For the scenario with  $B \gg B_C$ , the flow is believed to be dominated by thermal effects. It is worth noting that the suggested critical value is applicable to canyons of aspect ratios of 0.3–1.2.



**Fig. 9.** Canyon-wide circulation driven by both shear flow and thermal plume from a hot wall.  $T_h$  and  $T_l$  denote walls of high and low temperatures;  $U_T$  denotes the horizontal velocity driven by buoyancy effect and  $U_S$  denotes the horizontal velocity dominated by the incoming shear layer.

Other cases where the ground and/or windward wall are at higher temperature were also considered in Ref. [56]. It turns out that the heating of ground and leeward wall strengthens the canyon-wide circulation, whereas the windward wall at high temperature tends to create a counter-rotating vortex for cases at low Reynolds numbers. A more thorough discussion in this regard is presented below in section 3.2.1.

### 3.1.5. Sectional remarks

It has been challenging to theoretically analyse non-isothermal street canyon flows due to the complexity in the physical processes where a turbulent shear-layer flow and associated vortices, an impinging flow at the corner of the windward wall, upward buoyant layers adjacent to heated building walls and rising air parcels heated up by time-dependent solar radiation are present and in complex interaction. The scaling analysis that considers dominant heat transfer and momentum balances has been a promising approach to derive key velocity and temperature scales (correlations). Those scales are of great importance in the context of urban microclimate where large-scale flow motions and bulk temperatures are of primary interest.

Current scaling analyses certainly could be further extended to three-dimensional street canyon flows where multiple regimes of the in-canyon flow may be derived by considering the inflow from sides of buildings. Furthermore, existing studies have only been considering

constant heating. The contribution of momentum and heat from the buoyant layer(s) adjacent to heated building walls and grounds could be analysed on time-dependent basis for future research.

## 3.2. Experimental studies

Whilst some theoretical considerations devoted to thermal effects on street canyon flows, experimental studies also visited this topic. Among those experimental studies, some had well-defined thermal conditions while others were field measurements subjected to fluctuations in realistic microclimates. The review and discussion below are therefore grouped into these two categories. The configuration of street canyons is classified into '2D', '3D' and 'field' to represent 2D canyons, 3D canyons and field measurements, respectively, as noted in Table 3. In a 2D canyon, the effect of side flow into the canyon is isolated, which is the case of long canyons.

### 3.2.1. Street canyon flows subject to well-defined thermal conditions

Ref. [36] studied flows across a well-defined non-isothermal street canyon using a laser Doppler anemometer (LDA) in a wind tunnel setting. Buoyancy effects on street canyon flows were created and studied by controlling the freestream air and wind tunnel floor temperature separately. The thermal stratification decelerated the wind

**Table 3**  
Experimental studies on non-isothermal street canyon flows.

References	Canyon Config.	Heated surface(s)	Ri	A (H/W)	Exp. Approach <sup>a</sup>	Key words	Remarks
[84]	Field, Japan	N.A.	Meteorological condition	~1	TC, (FM)	Small air temperature difference	b
[162]	Field, Greece	N.A.	Meteorological condition	21/8.5	TM, LDA, (FM)	Deep pedestrian canyon	c
[36]	3D	Leeward wall	0.8 ~ -0.21	1	LDA, CW, (W)	Threshold of bulk Ri	d
[163]	Field, US	N.A.	Meteorological condition	~0.18	UA, FOQT, HW, MR, etc	Meteorological data and thermal mapping	e
[51]	2D	Windward wall	1/2.03, 1/1.17, 1/0.73	1	LDA, TC, (W)	Influence of buoyancy effects	f
[52]	Field, France	N.A.	Meteorological condition	21/14.85	TC, (FM)	Local effects of a thermal layer	g
[53]	2D	Ground	0, 10, 12.5, 20	0.67, 0.83, 1	PIV, (F)	Dominant flow structures	h
[164]	Field, Switzerland	N.A.	Meteorological condition	~1	WP, (FM)	Boundary layer structure in and over street canyons	i
[165]	Field, Sweden	N.A.	Meteorological condition	15/7.1	TC, UA, (FM)	Surface and air temperature rise	j
[166]	3D	N.A.	Meteorological condition	5/2	TC, (FM)	Boundary layer near façade	k
[56]	2D	Windward wall, leeward wall, ground	0.06-1.5	1	PIV, (W)	Low Froude numbers promote air exchange	l
[167]	3D	Ground, building walls	2.2-2.3, -3.0 ~ -2.9	0.96, 1.92	LDA, CW, (W)	Influence of thermal stratification	m
[57]	3D	Ground	1/8.34, 1/0.79, 1/0.30	~1	PIV, TC, (W)	Non-uniform building heights	n
[168]	3D	Roof, ground, leeward wall, windward wall	1.176, 0.131	1, 2, 0.67	PIV, TC, (W)	Different surface heating conditions	o

<sup>a</sup> (W) refers to wind tunnel measurements, (F) water tunnel (flume) measurements and (FM) field measurements. PIV refers to particle image velocimetry, TC the thermocouples, TM the thermistors, FOQT the fibreoptic-quartz thermometer, HW the hot wire, CW the cold wire, LDA the laser doppler anemometer, UA the ultrasonic anemometer, MR the microwave radiometer and WP the wind profiler.

<sup>b</sup> The temperature difference between air inside and outside the canyon was generally small, being less than 1 °C, except within 0.5 m from street or walls.

<sup>c</sup> The impact of canyon surface temperature resulted in up to 4.5 °C air temperature difference.

<sup>d</sup> A threshold of bulk Richardson number was determined to be 0.4–0.8, beyond which the wind speed at the street reduced to nearly zero.

<sup>e</sup> Meteorological and dispersion data were obtained from the mock urban setting test (MUST) project.

<sup>f</sup> The influence of the buoyancy forces induced by heating of a windward wall is limited within a very thin layer near the heat wall.

<sup>g</sup> A thin thermal layer developed closely adjacent to the heat wall, within a few centimetres from it.

<sup>h</sup> The ground heating facilitates the exchange of momentum and air mass between the ambient wind and flow inside the canyon.

<sup>i</sup> The Basel urban boundary layer experiment (BUBBLE) provides a year-long field measurement data which is useful for model evaluation.

<sup>j</sup> The canyon surface and air temperature rise were visualised and correlated.

<sup>k</sup> A thin thermal boundary layer of approximate 50 mm thickness was observed adjacent to the canyon surface.

<sup>l</sup> The air exchange of the street canyon is in general enhanced at low Froude numbers.

<sup>m</sup> Thermal stratification affects passive scalar diffusion substantially.

<sup>n</sup> Lateral flows could improve ventilation for a street canyon formed by buildings of different heights.

<sup>o</sup> The influence of surface heating at three different canyon aspect ratios was explored.

speed at the street level, whereas the circulation was enhanced when the wind tunnel floor temperature was higher than that of the freestream air. The threshold of the bulk Richardson number was correlated to be of  $Ri = 0.4 \sim 0.8$ . With a similar experimental configuration, Ref. [53] examined the problem with salt water in a static water chamber where the 'wind' was achieved by towing a heated box (measurement target). It was observed that the primary vortex shifted towards the leeward building as the wind speed increases.

Thermal effects from solar-induced windward wall were also examined by Ref. [51] using wind tunnel measurements. It was observed that the circulation of flow within the canyon weakens as the Froude number reduces from the neutral case. The reduction of circulation velocity at the street level was up to 50% due to the presence of the upward plume (a thermal boundary layer) from the heated windward wall, which decelerated the separated shear layer penetrating into the canyon.

A more recent study performed by Ref. [56] examined street canyon flows with various thermal conditions, from ground heating to wall heating and the combination of both. For all thermal conditions, thermal effects were found to be considerable at low  $Re$  ( $Re = 9000$ ), where buoyancy effects dominate the flow. When it comes to the flow at the maximum examined  $Re$  ( $Re = 30700$ ), effects of plumes from single or multiple heated surfaces can either suppress or enhance the flows, globally or locally.

Fig. 10 presents the measurement results of Ref. [56] where the first frame (Fig. 10a) presents a reference isothermal case. On one hand, it is clear that the cavity-wide circulation is suppressed due to the heating of the windward wall (Fig. 10b). The mechanism for this suppression is in line with that observed by Ref. [51]. On the other hand, the canyon flow is globally enhanced when the ground is heated up (Fig. 10c), whereas local enhancement is noted in the plume flowing adjacent to the leeward wall when it is at high temperature (Fig. 10d and e). These differences may be explained from the perspective of an effective Richardson number, though the bulk Richardson numbers of the four non-isothermal cases examined here are identical based on the temperature difference between a heated wall and far-field fluid. The underlying fact is that heat enters the canyon completely when the ground is at high temperature, whereas thermal effect is only present near the leeward wall when it is heated up. A considerable amount of heat is carried by the upward thermal boundary layer that leaves the canyon, suggesting that the bulk temperature of the fluid in the canyon is lower than that in the scenario with ground heating. How to characterise an effective Richardson number for street canyon flows with complex heating conditions is still an open question to the community.

The heating conditions and non-isothermal flow in each individual street canyon eventually contribute to the dynamics of the bulk flow in and above an urban area. In the case when street canyons are heated up higher than the mean temperature of upstream incoming flow, an unstable thermal stratification is created because the warmer layer of air beneath the urban canopy tends to flow upward due to buoyancy effect. Ref. [167] performed measurements of passive scalar diffusion under weakly stable and unstable thermal stratification conditions. It turned out that the unstable stratification promotes scalar diffusion

dramatically.

### 3.2.2. Street canyon flows measured in field

Flows in real street canyons are far more complex than those studied by laboratory measurements and numerical simulations. Real street canyon flows are affected by heterogeneous urban canopy, seasonal-dependent wind, diurnal and seasonal variation of solar radiation, vegetation and evapotranspiration, anthropogenic heat, human activities, etc. The complexity and heterogeneity of the topic was acknowledged in Ref. [169]. Field measurements is arguably the best way to obtain actual flow data that reflects influence of all factors. A detailed review of field measurements till 2004 is made by Ref. [82]. Recent field measurements were made by Refs. [106,170,171].

While the majority of field measurements were concerned with isothermal flow in real street canyons, some examined thermal effects on full-scale street canyon flows. The study by Ref. [84] revealed that a normal wall and floor absorb the most solar radiation on a site located in Kyoto, Japan ( $35^{\circ}00'N, 135^{\circ}45'E$ ). The temperature difference between air within and outside the street canyon was about  $0.5\text{--}1^{\circ}\text{C}$ . During daytime, surface temperature of a north façade directly exposed to solar radiation could be  $14^{\circ}\text{C}$  higher than that of a south façade.

Ref. [162] performed field measurements in a deep street canyon (height of 20 m and width of 8.5 m). A surface temperature difference of  $19^{\circ}\text{C}$  was recorded during a hot day. It also reported that the air temperature difference was up to  $3^{\circ}\text{C}$  along the canyon height direction and  $4.5^{\circ}\text{C}$  along the canyon width direction.

Another field measurement by Ref. [52] in Nantes, France, revealed the thermal layer from a heated wall. The width scale of the thermal layer was found to be up to 20 cm at a height of 12 m. Thermal effect is therefore thought to have local influence, which acts close to building walls [52]. A further discussion on local buoyant flows from the perspective of scaling analysis is presented in Section 4.1.

Temporal and spatial profiles of surface and air temperature in a real canyon due to solar radiation were visualised in Ref. [165]. The measurements were performed in central Gothenburg, Sweden, from July 2003 to August 2004. The canyon is 15 m high and 7.1 m wide. The temperature rise of canyon surfaces and in-canyon air was measured and estimated using the air temperature approximately 17 m above the roof level of the canyon as the reference temperature. It is seen in Fig. 11 that the surface temperature rise presents distinct temporal and spatial dependence. The most severe temperature rise occurred around noon time in the upper part of the canyon. This spatial feature was attributed to the sunlit profile. It is believed that the in-canyon flow circulation and turbulent mixing contributed to the complex pattern of air temperature rise. Similar findings were also obtained in an outdoor measurements within idealised canyons [166].

Other representative experimental studies on non-isothermal street canyon flows are summarised in Table 3. Key characteristics of those studies and their findings are also concluded.

### 3.2.3. Sectional remarks

Some experimental studies on non-isothermal street canyon flows

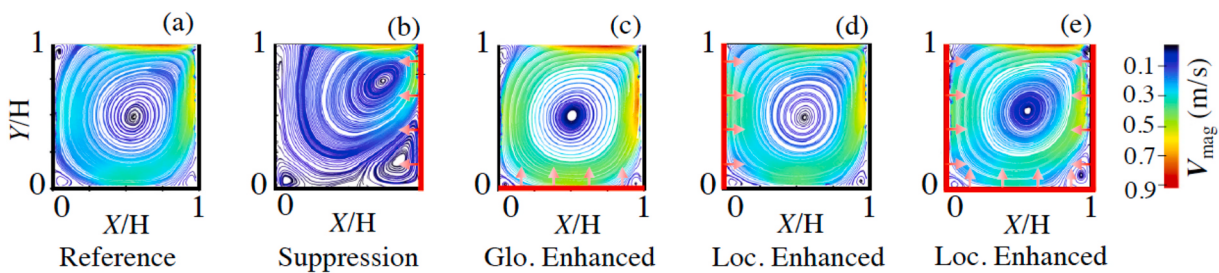


**Fig. 10.** Suppression or enhancement of circulation induced by surface heating,  $Re = 30700$  and  $Ri = 0.13$  (adapted from Ref. [56]). "Glo." and "Loc." are abbreviations for "globally/" and "locally". The red lines with arrows represent the heated surface(s) at constant temperature.

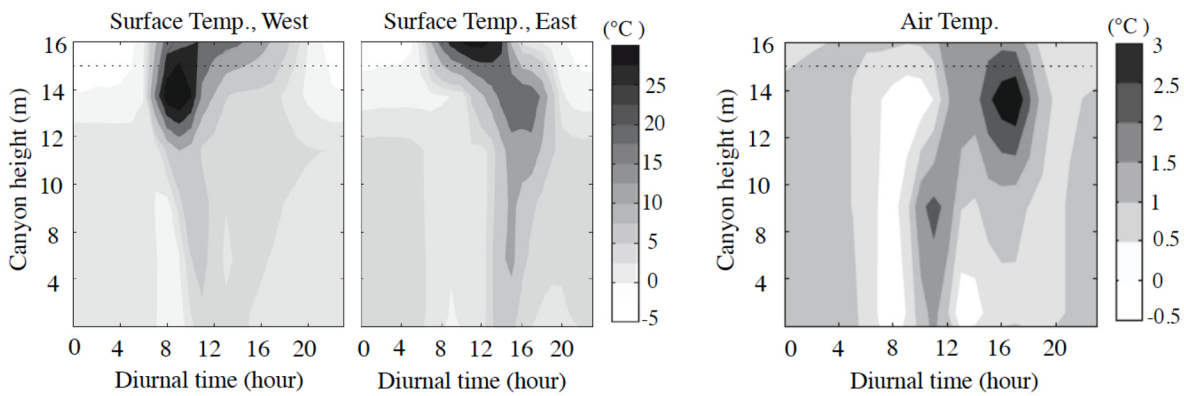


**Fig. 11.** Temperature rise of canyon surfaces and in-canyon air obtained from field measurements in central Gothenburg, Sweden, summer of July 2003–August 2004. Plots adapted from Ref. [165]. The dotted lines denote the roof level of the canyon.

have been implemented in the past and understanding of buoyancy effects have been obtained, mostly in regard to the strengthening or reduction in the canyon-wide flow circulation and resultant ventilation potential. As a generic understanding, thermal effects play a more important role at low wind speeds, i.e., low Reynolds numbers. The field measurements discovered local thermal effects which are mainly caused by solar radiation and heat absorption at the surface of building walls.

As the advancement of experimental techniques, such as laser induced fluorescence (LIF), non-isothermal street canyon flows can be better understood using current PIV and LIF measurements. Some interesting research questions that deserve experimental investigations include:

- time- and spatial-resolved PIV-LIF allowing to analyse the coupling of the flow and temperature fields of three-dimensional street canyon flows;
- scalar (e.g., heat, pollutant particles) transport and removal from street canyons to the urban canopy layer; and
- effects of surrounding greening on temperature field within a canyon.

### 3.3. Numerical simulations

Numerical simulations can model full-scale non-isothermal flows, thus satisfying all dimensionless parameters. Nevertheless, the abundance of reduced-scale experiments and the scarcity of full-scale measurements have driven the validation of most CFD models with reduced-scale experiments. The requirement of similarity criteria causes a bigger problem for buoyant flows in comparison to isothermal, or forced-convective cases [114]. Although the Froude number can be satisfied at reduced scale [38,56], the Reynolds number independence assumptions have been incorrectly generalised to non-isothermal flows [58]. This may produce wrong results and misleading conclusion for full-scale street canyons, especially for RANS simulations.

#### 3.3.1. Modelling of buoyancy

The flow field in a street canyon can show completely different characteristics due to buoyancy induced by high surface temperatures at the building façades, in some cases with additional vortices formed [51, 56,172]. In buoyancy-dominated flows with high building/ground surface temperatures and low wind speed, unsteadiness increases and turbulence generation due to buoyancy becomes significant. Therefore, care must be taken when choosing turbulence models for flows with reduced wind speed and reduced advective cooling. However, guidelines do not provide specific recommendations in regard to buoyancy modelling. It is a common practice to model buoyancy with the

Boussinesq approximation, which is only valid for small density changes in the flow field [173–175]. There are also examples, where density variation and related buoyancy effects are taken into account by an equation of state [45,176]. Furthermore, the commonly-used logarithmic inlet conditions by Ref. [177] are only valid for neutrally stratified isothermal ABL conditions. They can still be applicable in near-neutral conditions for non-isothermal simulations when temperature differences are not large enough to cause significant change in thermal stratification [178]. However, settings for computational domain and boundary conditions are not as straightforward for natural convection in the lack of a predominant wind flow.

#### 3.3.2. Modelling of wall heat transfer

At reduced scale, RANS generally performs well in simulating non-isothermal flows, with good agreement to experimental data [70,159, 179], but care should be taken for wall treatment. Ref. [180] showed that for bluff bodies, the impact of wall treatment for temperature is more significant than that for velocity field. Low Reynolds number modelling (LRNM) is more accurate compared to models that use standard wall functions [181], which often lead to inaccurate predictions of wall heat transfer [180]. This is mainly due to the fact that the standard wall functions are derived for wall-attached boundary layers under equilibrium conditions. Ref. [182] proposed an adjusted thermal wall function in non-equilibrium mixed convection conditions. Later, Ref. [183] extended this by dynamically switching wall functions based on local Richardson number and validated against wind-tunnel measurements in a street canyon.

Ref. [184] shows that convective heat transfer coefficients (CHTC) for street canyons are lower than those for isolated buildings due to lower wind speeds obtained in street canyons. In addition to the building geometry, the CHTC values depend on both wind speed and surface temperature when buoyancy is present. Typically CHTC values increase with wind speed, except at low wind speeds where buoyancy dominates and wall heat flux becomes constant.

At full scale, on the other hand, the use of LRNM is computationally expensive. Hence, most studies use wall functions, which may hinder the same level of accuracy [185]. Field measurements suggest that thermal effects are limited to a thin layer near the heated walls and are negligible in the overall flow field (a further discussion is presented in section 4). By contrast, RANS simulations at full scale predict strong thermal effects with significant alteration of the overall flow field, for instance, in Refs. [52,186,187]. One important aspect in non-isothermal cases is the temporal changes in the flow field caused by thermal effects, which are not captured by steady RANS [60,112,188].

One attempt on modelling heat transfer at walls was performed from the standpoint of surface energy balance. Ref. [189] presented a model

in which time-dependent longwave and shortwave radiation, conduction and convection were considered for heat transfer balance at surfaces. Ref. [44] also incorporated the Algebraic Wall-Modelled LES (WMLES) into the surface energy balance model and analysed the impact of heat transfer on ventilation. The WMLES provides a scale of wall-distance to switch from RANS to LES as grids are away from walls [190]. The latest work by Ref. [4] further examined coupled transport of heat and moisture (HAM) within porous urban materials, together with a CFD model of a street canyon where heat and moisture transport in air were modelled as an active and a passive scalar respectively.

The development of the algebraic-flux based three-equation ( $k - \varepsilon - \theta^2$ ) approach [191–193] within the framework of unsteady RANS model presents wall functions for the modelling of thermal convection over horizontal surfaces or realistic urban terrain. The introduction of the temperature variance  $\theta^2$ , in addition to the convective turbulence kinetic energy  $k$  and its dissipation rate  $\varepsilon$ , makes it possible to model near-wall turbulent heat transfer in a computationally-efficient way while being able to capture large scale flow structures.

On the other hand, LES gives inconclusive results, where full-scale LES could predict significant thermal effects [161] or negligible thermal effects [58]. Clearly, our understanding on non-isothermal flows is limited and much works needed to be done.

### 3.3.3. Sectional remarks

Numerical simulations of non-isothermal street canyon flows are challenging due to many uncertainties in the modelling process, such as buoyancy terms and wall heat transfer. The scaling mismatch adds another layer of complexity that even the state-of-the art LES models could produce contrasting results. We believe the thermal effects and scaling issue warrant a further discussion with fundamentals of fluid mechanics and heat transfer, which will be presented in section 4. On numerical modelling, research is still required for:

- improvement of thermal wall functions for mixed convective and buoyant flows in urban physics applications;
- extension of best-practice guidelines with respect to non-isothermal flows;
- analysis of unsteady thermal behaviour in buoyant cases with LES or hybrid URANS/LES; and
- further development of non-isotropic turbulence models within the framework of RANS and URANS.

## 4. Discussion on roles of buoyancy effects

### 4.1. Local buoyant flows

When it comes to solar-radiation induced thermal effects on flow dynamics and dispersion of pollutant within a street canyon, the above review has implied that laboratory studies, computational simulations and field measurements have led to different perspectives whether thermal effects are important. On one hand, field measurements [36, 165, 166] and numerical studies [58] at full scale have pointed out that thermal boundary layers induced by one or more heated walls do not play a significant role in the primary vortex structure. On the other hand, experimental results at reduced scale [51, 56] observed a distinct thermal boundary layer from a heated wall, which substantially suppressed the formation of the primary circulation flow.

In a long street canyon where lateral side inflow can be neglected, a fundamental cause leading to this discrepancy is the nonlinear growth of the thermal boundary layer thickness along a heated wall. The schematic shown in Fig. 8 illustrates the streamwise growth of a typical thermal boundary layer, at the scale up to typical heights of buildings. While laboratory studies scale down the measurement models by keeping the same aspect ratio  $A = 1$ , the thermal boundary layer thickness does not scale down linearly. To illustrate this point explicitly,

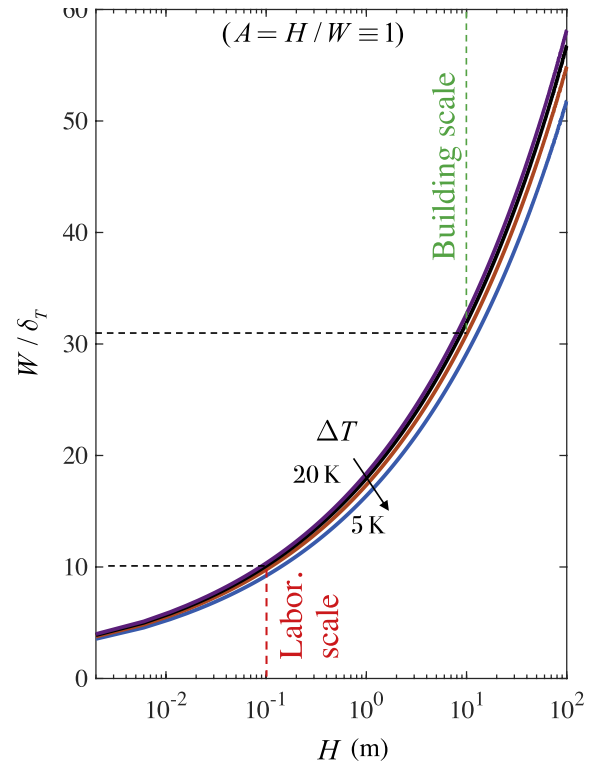


**Fig. 12.** The ratio between canyon width and thermal boundary layer thickness, at laboratory and building scales. Four curves represent estimations with wall-to-air temperature difference of 5, 10, 15 and 20 K, respectively.

we estimate the ratio between the street canyon width and the thickness of the thermal boundary layer induced by the heated wall, as a function of the height of the building (as shown in Fig. 12). The thickness of the thermal boundary layer,  $\delta_T$ , is estimated by the scales (correlations) given below:

$$\delta_T \sim \omega \frac{Gr_Y^{1/4} \nu}{(ga\Delta T \nu)^{1/3}}, \quad (15)$$

$$Gr_Y \sim \frac{ga\Delta TH^3}{\nu^2}, \quad (16)$$

where  $\omega$  is a coefficient of 0.331,  $Gr_Y$  the Grashof number determined based on the height of the wall ( $H$ ) and  $\alpha$  the coefficient of thermal expansion. In correlation (16),  $g$ ,  $\nu$  and  $\Delta T$  denote the gravity, kinematic viscosity and temperature difference between the wall and far-field ambient fluid. This estimation was given by Ref. [194]; which is also in a reasonable agreement with the recent results derived by Ref. [160]; as reviewed above.

It is seen in Fig. 12 that at typical laboratory scale where the height of a building model is around  $10^{-1}$  m, the ratio  $W/\delta_T$  is about 10. This means 1/10 of a street canyon is occupied by the thermal layer. On the other hand, when it comes to a building scale, for instance a building of 10 m, the ratio  $W/\delta_T$  increases to above 30. For a typical building with a height of 10–100 m, the ratio spans 30–58. It is immediately clear that the presence of the thermal layer does not affect the primary circulation in the centre of a tall full-scale canyon. The thermal effects become less significant with increasing canyon height  $H$ .

Fig. 12 only examines  $W/\delta_T$  for canyons with  $H/W = 1$ . The thermal effects can become significant if the canyon has large  $H/W$ , i.e., narrow canyons, which are common in high density cities, for instance Hong Kong and Singapore. The ratio of  $W/\delta_T$  would reduce to about 10 in a

canyon of 10 m height and 3 m width. For narrow canyons receiving less solar radiation due to shadowing, the waste heat discharged to a canyon from air-conditioners along the height of building façades may result in significant buoyant flows.

From the perspective of pollutant dispersion, thermal plumes from one or more heated walls and/or ground may play a dramatic role, depending on the location and spatial distribution of pollutant sources [50]. If a pollutant source is located near building walls, upward thermal plumes would facilitate the dispersion outside the street canyon. A common example of this scenario is pollutant from venting system that is directly exposed to a canyon through opening of building walls.

#### 4.2. Non-neutral approaching urban boundary layer

Apart from influence of thermal effects induced by buildings, thermal stratification of the urban boundary layer also plays a role in street canyon flows, in particular to passive scalar dispersion. A few studies on non-neutral urban boundary layer and the resultant effect on passive scalar diffusion were conducted recently by Refs. [167,195–198]. The case of an approaching urban boundary layer, which is at a temperature lower than the urban area of interest, is referred to as either an unstable thermal stratification [195] or a convective atmospheric condition [197]. A stable thermal stratification usually refers to the case that the mean temperature of an approaching boundary layer is higher than that of the urban area immersed in it [198].

The LES in Ref. [195] suggested that effects of thermal stratification on dispersion in urban environments are not negligible. This point was also claimed in a wind tunnel study of Ref. [167] in which the effects of purposely created stable and unstable thermal stratification were explored. The trials of creating a thick non-neutral boundary layer with a good lateral uniformity in wind tunnel were reported in Ref. [196]. The influences of various characteristics of the approaching convective (unstable) boundary layer, such as inlet temperature, turbulent quantities and heat fluxes, were also examined. A continued wind tunnel study of the same group [197] found that dispersion can be promoted up to three times higher by the convective boundary layer compared to that in the neutral case. This is in line with the finding of Ref. [198] in which a greater stable thermal stratification of an approaching urban boundary layer was found to suppress passive scalar dispersion due to the reduced turbulence and vertical convective flux in the urban boundary layer, as shown in Fig. 13.

## 5. Emerging approaches for passive scalar dispersion by street canyon flows

Full-scale three-dimensional street canyon flows are more complex where side airflow around street canyon corners induce vortices. The penetration of these vortices into a canyon centre depends on geometrical and aerodynamic factors [71,199]. Also, when it comes to the modelling of a large number of street canyons, a resultant large computational domain and flow structures at various scales challenge numerical simulations using conventional RANS or LES. Some emerging approaches with new concepts have been explored for passive scalar dispersion in full-scale three-dimensional flows, which are briefly reviewed below.

### 5.1. Street network model

Street network model [200–202] is mainly developed to understand scalar dispersion through city centres where airspace of street canyons is divided into boxes for subsequent turbulence rendering. The superiority of the street network model is its analytical solution which is a function of three parameters: plume direction, transmission and a normalised source strength [201]. However, the validity of such a model is found to be sensitive to the wind direction [201,202]. Remedies need to be taken when the wind direction closely aligns with one of the axes of the network.

### 5.2. Wavelet-based homogenisation

Multiscale numerical methods for passive advection-diffusion in turbulent flows are receiving more research interest [203]. A recent study by Ref. [204] introduced a systematic approach for parameterising scalar dispersion at subgrid-scale, which may be viewed as a higher-order averaging theory. The contribution of the work lies in that it provides an intermediate numerical tool to combine the scales resolved by CFD and atmospheric modelling. As pointed out in Ref. [204]; empirical parameterisations for larger and realistic urban domains could be expected from this approach.

### 5.3. Mixed porous model

In the mixed porous model part of a target urban area is modelled as a porous medium [205–207] whereas flow around buildings of interest is fully resolved using CFD [208]. This model makes it possible to

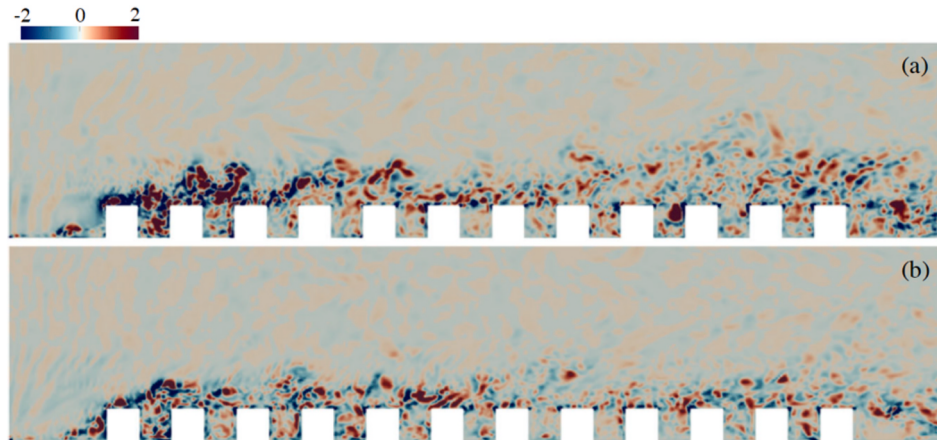


**Fig. 13.** Q-criterion contours showing the flow in and above the canon with approaching urban boundary layer (a) at  $Ri = 0.21$  (relatively weak thermal stratification) and (b)  $Ri = 1$  (relatively strong thermal stratification), adapted from Ref. [198].

simulate a large urban area while maintaining sufficient resolution for regions where detailed flow characteristics are important. Interestingly, this type of model may also be adopted in combination of city-scale models to study urban heat island effects [209].

## 6. Concluding remarks

We have reviewed advances of studies on street canyon flows, from theoretical modelling to experimental studies and recent numerical simulations. The review covered both isothermal and non-isothermal street canyon flows. Also, the conditions in which thermal effects play a vital role are discussed.

The present paper reviews theoretical models of street canyons with simplified geometries allowing analyses of the main physical mechanisms at play. Those theoretical models consider two-dimensional canyons and two-dimensional flows. In wind tunnel or water tunnel experiments, geometrical and aerodynamic restrictions of the theoretical models can be relaxed. These experimental studies are mostly concerned with three-dimensional street canyon flows generated in two-dimensional cavities or from an array of cubes, while only a limited number of studies use realistic physical models down-scaled to neighbourhood-scale. Limitation of experimental studies lies in that the approach flow can only be mimicked according to simplified profile of local wind at specific speed and direction. By contrast, CFD models enjoy more capabilities and freedom to model and analyse street canyon flows at actual neighbourhood-scale with meteorological wind data.

From a theoretical point of view, a street canyon flow is a complex flow where multiple mechanisms drive the flow dynamics, from wall-jet like shear layer flow at the top of a canyon to the impingement of the shear layer and later boundary-layer-like flow along building surfaces. Thanks to some modelling works, primary flow dynamics of street canyon flows can be estimated. When thermal effects from either heated walls or ground come into play, the dynamics become even more complex. Some scales for key characteristics of flow circulation in full-scale canyons are identified.

Reduced-scale laboratory measurements have been a vital approach to this field, though a full set of similarities to a field setting cannot be always achieved. Primary flow dynamics of street canyon flows have been understood through wind tunnel and water tunnel measurements. The separated shear flow and the primary vortex have been observed in various measurements, which are accurately predicted by numerical simulations. To study thermal effects on street canyon flows, measurements have been conducted with controlled surface temperature of building models. It turned out that a heated windward wall would significantly weaken canyon-wide flow circulation. However, this flow weakening was not seen in some field measurements with full-scale canyons. The fact is that the thickness of the thermal boundary layer (plume) adjacent to a heated wall does not grow linearly with the height of the wall. In full-scale canyons, the plume plays a significant role in localised regions adjacent to the heated walls. Caution needs to be exercised to compare between reduced-scale experiments and field measurements.

While wind tunnel experiments suffer from scale mismatch, CFD simulations can model full-scale canyons, as there is no size limit to the computational domain. CFD simulations also allow full control of the canyon geometry and the boundary conditions, thus making it a suitable tool for parametric studies such as canyon aspect ratio and wind direction. Nevertheless, CFD simulations should not be a stand-alone tool and should always be validated with measurements from experiments or field studies. CFD simulations with validation from experiments have been the most common method, as this coupling combines the strengths of both methods while complementing the drawback of each other.

Further development of numerical modelling is also much needed, especially for non-isothermal urban street canyon flows. Improvements in wall treatment for accurate near-wall heat transfer and in buoyancy modelling for buoyancy-dominated flows (e.g., turbulence generation

due to buoyancy) are required for full-scale urban modelling. Additionally, best-practice guidelines should be extended accordingly for buoyancy-dominated flows (natural convection) in terms of domain size, boundary conditions and turbulence modelling. In the context of urban microclimate where both large-scale coherent flow structures and mean flow characteristics are of primary interest, computationally efficient unsteady turbulence models with high accuracy are expected to be developed. The advances in reduced order modelling (ROM) may bring opportunities to fast and efficient numerical simulations of non-isothermal flows to the urban microclimate community.

Modelling of real street canyon flows, taking into account heterogeneous urban canopy, time dependent wind, solar radiation and rain, vegetation and evapotranspiration, anthropogenic heat and human activities, is an interdisciplinary research topic. The model accuracy depends on the correct modelling capabilities of each of these physical processes and how they are coupled. Towards high-resolution real street canyon flow simulation, there are still many challenging research questions, such as (1) high-resolution modelling of vegetation and evapotranspiration effects in street canyons, (2) modelling of time-dependent anthropogenic heat in street canyons or in near street canyon regions, (3) high-resolution modelling of thermal feedback of building materials to longwave and shortwave radiation, (4) modelling of aerodynamic influence of human activities (pedestrians, cars, etc) in street canyons, (5) high-resolution blending of inflow boundary conditions from mesoscale meteorological models, (6) parametrization of urban canopies, (7) high-resolution laboratory measurements of street canyon flows involving multiple physical processes for model validation, (8) long-term field measurements to distinguish dominating physical mechanisms, and (9) coupling of validated ‘sub-models’ of dominating physical processes.

## Declaration of competing interest

The authors declare that they have no known competing financial interests or personal relationships that could have appeared to influence the work reported in this paper.

## Acknowledgements

The support by the Swiss National Science Foundation (SNF 200021–169323) and the Chair of Building Physics at the ETH Zürich is greatly appreciated. We also thank L. Soulhac, F. Caton, Y. Bengana, E. Paterna, Z.T. Xie, B. Offerle and J. Allegrini for their permission to adopt their figures in publication.

## References

- [1] R. Emmanuel, E. Krüger, Urban heat island and its impact on climate change resilience in a shrinking city: the case of Glasgow, UK, *Build. Environ.* 53 (2012) 137–149.
- [2] L.O. Myrup, A numerical model of the urban heat island, *J. Appl. Meteorol.* 8 (1969) 908–918.
- [3] T.R. Oke, Review of Urban Climatology. Technical Note No. 169, Secretariat of the World Meteorological Organization, Geneva, Switzerland, 1979.
- [4] A. Kubilay, D. Derome, J. Carmeliet, Impact of evaporative cooling due to wetting of urban materials on local thermal comfort in a street canyon, *Sustainable Cities and Society* 49 (2019) 101574.
- [5] A. Ferrari, A. Kubilay, D. Derome, J. Carmeliet, The use of permeable and reflective pavements as a potential strategy for urban heat island mitigation, *Urban Climate* 31 (2020) 100534.
- [6] H. Taha, H. Akbari, A. Rosenfeld, J. Huang, Residential cooling loads and the urban heat island—the effects of albedo, *Build. Environ.* 23 (1988) 271–283.
- [7] H. Taha, Urban climates and heat islands: albedo, evapotranspiration, and anthropogenic heat, *Energy Build.* 25 (1997) 99–103.
- [8] F. Salata, I. Golasi, A.d.L. Vollaro, R.d.L. Vollaro, How high albedo and traditional buildings' materials and vegetation affect the quality of urban microclimate. A case study, *Energy Build.* 99 (2015) 32–49.
- [9] J. Yuan, C. Farnham, K. Emura, Development of a retro-reflective material as building coating and evaluation on albedo of urban canyons and building heat loads, *Energy Build.* 103 (2015) 107–117.
- [10] J. Deng, B.J. Pickles, A. Kavakopoulos, T. Blanusa, C.H. Halias, S.T. Smith, L. Shao, Concept and methodology of characterising infrared radiative

- performance of urban trees using tree crown spectroscopy, *Build. Environ.* 157 (2019) 380–390.
- [11] A. Kubilay, D. Derome, B. Blocken, J. Carmeliet, CFD simulation and validation of wind-driven rain on a building facade with an Eulerian multiphase model, *Build. Environ.* 61 (2013) 69–81.
- [12] A. Kubilay, D. Derome, B. Blocken, J. Carmeliet, Numerical simulations of wind-driven rain on an array of low-rise cubic buildings and validation by field measurements, *Build. Environ.* 81 (2014) 283–295.
- [13] A. Kubilay, D. Derome, B. Blocken, J. Carmeliet, High-resolution field measurements of wind-driven rain on an array of low-rise cubic buildings, *Build. Environ.* 78 (2014) 1–13.
- [14] B. Blocken, J. Carmeliet, Impact, runoff and drying of wind-driven rain on a window glass surface: numerical modelling based on experimental validation, *Build. Environ.* 84 (2015) 170–180.
- [15] D. Derome, A. Kubilay, T. Defraeye, B. Blocken, J. Carmeliet, Ten questions concerning modeling of wind-driven rain in the built environment, *Build. Environ.* 114 (2017) 495–506.
- [16] M.A. Rahman, A. Moser, T. Rötzer, S. Pauleit, Within canopy temperature differences and cooling ability of *Tilia cordata* trees grown in urban conditions, *Build. Environ.* 114 (2017) 118–128.
- [17] M. Vuckovic, K. Kiesel, A. Mahdavi, Studies in the assessment of vegetation impact in the urban context, *Energy Build.* 145 (2017) 331–341.
- [18] L. Manickathan, T. Defraeye, J. Allegrini, D. Derome, J. Carmeliet, Parametric study of the influence of environmental factors and tree properties on the transpirative cooling effect of trees, *Agric. For. Meteorol.* 248 (2018) 259–274.
- [19] L. Manickathan, T. Defraeye, J. Allegrini, D. Derome, J. Carmeliet, Comparative study of flow field and drag coefficient of model and small natural trees in a wind tunnel, *Urban For. Urban Green.* 35 (2018) 230–239.
- [20] Y. Yang, E. Gatto, Z. Gao, R. Buccolieri, T.E. Morakinyo, H. Lan, The “plant evaluation model” for the assessment of the impact of vegetation on outdoor microclimate in the urban environment, *Build. Environ.* 159 (2019) 106151.
- [21] J.A. Fletcher, T. Kershaw, G. Mills, Urban form and function as building performance parameters, *Build. Environ.* 62 (2013) 112–123.
- [22] W.-S. Nie, T. Sun, G.-H. Ni, Spatiotemporal characteristics of anthropogenic heat in an urban environment: a case study of Tsinghua Campus, *Build. Environ.* 82 (2014) 675–686.
- [23] M. Ichinose, T. Inoue, T. Nagahama, Effect of retro-reflecting transparent window on anthropogenic urban heat balance, *Energy Build.* 157 (2017) 157–165.
- [24] J. Yang, K.W. Tham, S.E. Lee, M. Santamouris, C. Sekhar, D.K.W. Cheong, Anthropogenic heat reduction through retrofitting strategies of campus buildings, *Energy Build.* 152 (2017) 813–822.
- [25] Y. Fan, Y. Li, S. Yin, Interaction of multiple urban heat island circulations under idealised settings, *Build. Environ.* 134 (2018) 10–20.
- [26] Y. Fan, Y. Li, S. Yin, Non-uniform ground-level wind patterns in a heat dome over a uniformly heated non-circular city, *Int. J. Heat Mass Tran.* 124 (2018) 233–246.
- [27] A.S. Adelia, C. Yuan, L. Liu, R.Q. Shan, Effects of urban morphology on anthropogenic heat dispersion in tropical high-density residential areas, *Energy Build.* 186 (2019) 368–383.
- [28] F. Yang, S.S.Y. Lau, F. Qian, Summertime heat island intensities in three high-rise housing quarters in inner-city Shanghai China: building layout, density and greenery, *Build. Environ.* 45 (2010) 115–134.
- [29] J. Niu, J. Liu, T.-c. Lee, Z. Lin, C. Mak, K.-T. Tse, B.-s. Tang, K.C.S. Kwok, A new method to assess spatial variations of outdoor thermal comfort: onsite monitoring results and implications for precinct planning, *Build. Environ.* 91 (2015) 263–270.
- [30] J. Allegrini, J. Carmeliet, Coupled CFD and building energy simulations for studying the impacts of building height topology and buoyancy on local urban microclimates, *Urban Climate* 21 (2017) 278–305.
- [31] Y. Du, C.M. Mak, J. Liu, Q. Xia, J. Niu, K.C.S. Kwok, Effects of lift-up design on pedestrian level wind comfort in different building configurations under three wind directions, *Build. Environ.* 117 (2017) 84–99.
- [32] J. Liu, J. Niu, C.M. Mak, Q. Xia, Detached eddy simulation of pedestrian-level wind and gust around an elevated building, *Build. Environ.* 125 (2017) 168–179.
- [33] J. Liu, J. Niu, Delayed detached eddy simulation of pedestrian-level wind around a building array – the potential to save computing resources, *Build. Environ.* 152 (2019) 28–38.
- [34] J. Liu, X. Zhang, J. Niu, K.T. Tse, Pedestrian-level wind and gust around buildings with a ‘lift-up’ design: Assessment of influence from surrounding buildings by adopting LES, *Building Simulation* 12 (2019) 1107–1118.
- [35] D.O. Lee, Rural atmospheric stability and the intensity of London’s heat island, *Weather* 30 (1975) 102–109.
- [36] K. Uehara, S. Murakami, S. Oikawa, S. Wakamatsu, Wind tunnel experiments on how thermal stratification affects flow in and above urban street canyons, *Atmos. Environ.* 34 (2000) 1553–1562.
- [37] A. Dallman, S. Magnusson, R. Bitter, L. Norford, D. Entekhabi, H.J.S. Fernando, Conditions for thermal circulation in urban street canyons, *Build. Environ.* 80 (2014) 184–191.
- [38] S. Magnusson, A. Dallman, D. Entekhabi, R. Bitter, H.J.S. Fernando, L. Norford, On thermally forced flows in urban street canyons, *Environ. Fluid Mech.* 14 (2014) 1427–1441.
- [39] J.-F. Sini, S. Anquetin, P.G. Mestayer, Pollutant dispersion and thermal effects in urban street canyons, *Atmos. Environ.* 30 (1996) 2659–2677.
- [40] X.-X. Li, C.-H. Liu, D.Y.C. Leung, Large-eddy simulation of flow and pollutant dispersion in high-aspect-ratio urban street canyons with wall model, *Boundary-Layer Meteorol.* 129 (2008) 249–268.
- [41] J. Hang, Y. Li, Age of air and air exchange efficiency in high-rise urban areas and its link to pollutant dilution, *Atmos. Environ.* 45 (2011) 5572–5585.
- [42] J. Hang, Y. Li, M. Sandberg, R. Buccolieri, S. Di Sabatino, The influence of building height variability on pollutant dispersion and pedestrian ventilation in idealized high-rise urban areas, *Build. Environ.* 56 (2012) 346–360.
- [43] H. Kikumoto, R. Oooka, Large-eddy simulation of pollutant dispersion in a cavity at fine grid resolutions, *Build. Environ.* 127 (2018) 127–137.
- [44] N. Nazarian, J. Kleissl, Realistic solar heating in urban areas: Air exchange and street-canyon ventilation, *Build. Environ.* 95 (2016) 75–93.
- [45] K. Javanroodi, M. Mahdavinejad, V.M. Nik, Impacts of urban morphology on reducing cooling load and increasing ventilation potential in hot-arid climate, *Appl. Energy* 231 (2018) 714–746.
- [46] Z. Mo, C.-H. Liu, A wind tunnel study of ventilation mechanism over hypothetical urban roughness: the role of intermittent motion scales, *Build. Environ.* 135 (2018) 94–103.
- [47] Z. Li, T. Shi, Y. Wu, H. Zhang, Y.-H. Juan, T. Ming, N. Zhou, Effect of traffic tidal flow on pollutant dispersion in various street canyons and corresponding mitigation strategies, *Energy and Built Environment* 1 (2020) 242–253.
- [48] Y. Peng, R. Buccolieri, Z. Gao, W. Ding, Indices employed for the assessment of “urban outdoor ventilation” - a review, *Atmos. Environ.* 223 (2020) 117211.
- [49] T.R. Oke, Street design and urban canopy layer climate, *Energy Build.* 11 (1988) 103–113.
- [50] J.-J. Kim, J.-J. Baik, A numerical study of thermal effects on flow and pollutant dispersion in urban street canyons, *J. Appl. Meteorol.* 38 (1999) 1249–1261.
- [51] A. Kovar-Panskus, L. Moulinneuf, E. Savory, A. Abdelqari, J.-F. Sini, J.-M. Rosant, A. Robins, N. Toy, A wind tunnel investigation of the influence of solar-induced wall-heating on the flow regime within a simulated urban street canyon, *Water, Air and Soil Pollution: Focus* 2 (2002) 555–571.
- [52] P. Louka, G. Vachon, J.-F. Sini, P.G. Mestayer, J.-M. Rosant, Thermal effects on the airflow in a street canyon – nantes’99 experimental results and model simulations, *Water Air Soil Pollut. Focus* 2 (2002) 351–364.
- [53] H. Liu, B. Liang, F. Zhu, B. Zhang, J. Sang, A Laboratory model for the flow in urban street canyons induced by bottom heating, *Adv. Atmos. Sci.* 20 (2003) 554.
- [54] X. Xie, Z. Huang, J. Wang, Z. Xie, The impact of solar radiation and street layout on pollutant dispersion in street canyon, *Build. Environ.* 40 (2005) 201–212.
- [55] X. Xie, C.-H. Liu, D.Y.C. Leung, M.K.H. Leung, Characteristics of air exchange in a street canyon with ground heating, *Atmos. Environ.* 40 (2006) 6396–6409.
- [56] J. Allegrini, V. Dorer, J. Carmeliet, Wind tunnel measurements of buoyant flows in street canyons, *Build. Environ.* 59 (2013) 315–326.
- [57] J. Allegrini, A wind tunnel study on three-dimensional buoyant flows in street canyons with different roof shapes and building lengths, *Build. Environ.* 143 (2018) 71–88.
- [58] L.W. Chew, L.R. Glicksman, L.K. Norford, Buoyant flows in street canyons: comparison of RANS and LES at reduced and full scales, *Build. Environ.* 146 (2018) 77–87.
- [59] I.Y. Lee, H.M. Park, Parameterization of the pollutant transport and dispersion in urban street canyons, *Atmos. Environ.* 28 (1994) 2343–2349.
- [60] J.-J. Baik, J.-J. Kim, A numerical study of flow and pollutant dispersion characteristics in urban street canyons, *J. Appl. Meteorol.* 38 (1999) 1576–1589.
- [61] H. Huang, Y. Akutsu, M. Arai, M. Tamura, A two-dimensional air quality model in an urban street canyon: evaluation and sensitivity analysis, *Atmos. Environ.* 34 (2000) 689–698.
- [62] X.-X. Li, C.-H. Liu, D.Y.C. Leung, Development of a k- $\epsilon$  model for the determination of air exchange rates for street canyons, *Atmos. Environ.* 39 (2005) 7285–7296.
- [63] R.A. Memon, D.Y.C. Leung, C.-H. Liu, Effects of building aspect ratio and wind speed on air temperatures in urban-like street canyons, *Build. Environ.* 45 (2010) 176–188.
- [64] J. Hang, Y. Li, R. Buccolieri, M. Sandberg, S. Di Sabatino, On the contribution of mean flow and turbulence to city breathability: the case of long streets with tall buildings, *Sci. Total Environ.* 416 (2012) 362–373.
- [65] D. Cui, G. Hu, Z. Ai, Y. Du, C.M. Mak, K. Kwok, Particle image velocimetry measurement and CFD simulation of pedestrian level wind environment around U-type street canyon, *Build. Environ.* 154 (2019) 239–251.
- [66] J. Liu, J. Niu, Q. Xia, Combining measured thermal parameters and simulated wind velocity to predict outdoor thermal comfort, *Build. Environ.* 105 (2016) 185–197.
- [67] L.W. Chew, L.K. Norford, Pedestrian-level wind speed enhancement with void decks in three-dimensional urban street canyons, *Build. Environ.* 155 (2019) 399–407.
- [68] D. Marucci, M. Carpentieri, Effect of local and upwind stratification on flow and dispersion inside and above a bi-dimensional street canyon, *Build. Environ.* 156 (2019) 74–88.
- [69] H.J.S. Fernando, D. Zajic, S.D. Sabatino, R. Dimitrova, B. Hedquist, A. Dallman, Flow, turbulence, and pollutant dispersion in urban atmospheres, *Phys. Fluids* 22 (2010), 051301.
- [70] P.-Y. Cui, Z. Li, W.-Q. Tao, Wind-tunnel measurements for thermal effects on the air flow and pollutant dispersion through different scale urban areas, *Build. Environ.* 97 (2016) 137–151.
- [71] L.J. Hunter, G.T. Johnson, I.D. Watson, An investigation of three-dimensional characteristics of flow regimes within the urban canyon, *Atmos. Environ. Part B - Urban Atmos.* 26 (1992) 425–432.
- [72] F. Pan, A. Acrivos, Steady flows in rectangular cavities, *J. Fluid Mech.* 28 (1967) 643–655.
- [73] E. Paterna, Wind Tunnel Investigation of Turbulent Flow in Urban Configurations: a Time - Resolved PIV Analysis, Ph.D Thesis, ETH Zurich, 2015.

- [74] L. Soulhac, Modélisation de la dispersion atmosphérique à l'intérieur de la canopée urbaine, PhD Thesis, Ecole Centrale de Lyon tel., 2000, 01727430.
- [75] Y. Bengana, J.C. Loiseau, J.C. Robinet, L.S. Tuckerman, Bifurcation analysis and frequency prediction in shear-driven cavity flow, *J. Fluid Mech.* 875 (2019) 725–757.
- [76] J.-C. Lin, D. Rockwell, Organized oscillations of initially turbulent flow past a cavity, *AIAA J.* 39 (2001) 1139–1151.
- [77] W. Kang, H.J. Sung, Large-scale structures of turbulent flows over an open cavity, *J. Fluid Struct.* 25 (2009) 1318–1333.
- [78] M. Kawaguti, Numerical solution of the Navier-Stokes equations for the flow in a two-dimensional cavity, *J. Phys. Soc. Jpn.* 16 (1961) 2307–2315.
- [79] O.R. Burggraf, Analytical and numerical studies of the structure of steady separated flows, *J. Fluid Mech.* 24 (1966) 113–151.
- [80] F. Caton, R.E. Britter, S. Dalziel, Dispersion mechanisms in a street canyon, *Atmos. Environ.* 37 (2003) 693–702.
- [81] X.-X. Li, C.-H. Liu, D.Y.C. Leung, K.M. Lam, Recent progress in CFD modelling of wind field and pollutant transport in street canyons, *Atmos. Environ.* 40 (2006) 5640–5658.
- [82] I. Eliasson, B. Offerle, C.S.B. Grimmond, S. Lindqvist, Wind fields and turbulence statistics in an urban street canyon, *Atmos. Environ.* 40 (2006) 1–16.
- [83] N. Rajaratnam, Turbulent Jets, Elsvier Amsterdam, New York, 1976.
- [84] Y. Nakamura, T.R. Oke, Wind, temperature and stability conditions in an east-west oriented urban canyon, *Atmos. Environ.* 22 (1988) 2691–2700, 1967.
- [85] J.-J. Kim, J.-J. Baik, Urban street-canyon flows with bottom heating, *Atmos. Environ.* 35 (2001) 3395–3404.
- [86] S.E. Nicholson, A pollution model for street-level air, *Atmos. Environ.* 9 (1975) 19–31, 1967.
- [87] W. Kang, S.B. Lee, H.J. Sung, Self-sustained oscillations of turbulent flows over an open cavity, *Exp. Fluid* 45 (2008) 693.
- [88] J. Basley, L.R. Pastur, F. Lusseyran, T.M. Faure, N. Delprat, Experimental investigation of global structures in an incompressible cavity flow using time-resolved PIV, *Exp. Fluid* 50 (2011) 905–918.
- [89] M. Immer, J. Allegrini, J. Carmeliet, Time-resolved and time-averaged stereo-PIV measurements of a unit-ratio cavity, *Exp. Fluid* 57 (2016) 101.
- [90] Y.P. Tang, D. Rockwell, Instantaneous pressure fields at a corner associated with vortex impingement, *J. Fluid Mech.* 126 (1983) 187–204.
- [91] Z. Cui, X. Cai, C.J. Baker, Large-eddy simulation of turbulent flow in a street canyon, *Q. J. R. Meteorol. Soc.* 130 (2004) 1373–1394.
- [92] W.C. Cheng, C.-H. Liu, Large-eddy simulation of flow and pollutant transports in and above two-dimensional idealized street canyons, *Boundary-Layer Meteorol.* 139 (2011) 411–437.
- [93] L.W. Chew, A.A. Alabadi, L.K. Norford, Flows across high aspect ratio street canyons: Reynolds number independence revisited, *Environ. Fluid Mech.* 18 (2018) 1275–1291.
- [94] G. Ashcroft, X. Zhang, Vortical structures over rectangular cavities at low speed, *Phys. Fluids* 17 (2005), 015104.
- [95] C. Haigermoser, L. Vesely, M. Novara, M. Onorato, A time-resolved particle image velocimetry investigation of a cavity flow with a thick incoming turbulent boundary layer, *Phys. Fluids* 20 (2008) 105101.
- [96] R. Kellnerová, L. Kučáka, K. Jurčáková, V. Uruba, Z. Jaňour, PIV measurement of turbulent flow within a street canyon: detection of coherent motion, *J. Wind Eng. Ind. Aerod.* 104–106 (2012) 302–313.
- [97] F. Gerdes, D. Olivari, Analysis of pollutant dispersion in an urban street canyon, *J. Wind Eng. Ind. Aerod.* 82 (1999) 105–124.
- [98] J.-J. Baik, R.-S. Park, H.-Y. Chun, J.-J. Kim, A laboratory model of urban street-canyon flows, *J. Appl. Meteorol.* 39 (2000) 1592–1600.
- [99] X.-X. Li, D.Y.C. Leung, C.-H. Liu, K.M. Lam, Physical modeling of flow field inside urban street canyons, *J. Appl. Meteorol. Climatol.* 47 (2008) 2058–2067.
- [100] P. Salizoni, L. Soulhac, P. Mejean, R.J. Perkins, Influence of a two-scale surface roughness on a neutral turbulent boundary layer, *Boundary-Layer Meteorol.* 127 (2008) 97–110.
- [101] A. Inagaki, M. Kanda, Turbulent flow similarity over an array of cubes in near-neutrally stratified atmospheric flow, *J. Fluid Mech.* 615 (2008) 101–120.
- [102] M.K.-A. Neophytou, C.N. Markides, P.A. Fokaides, An experimental study of the flow through and over two dimensional rectangular roughness elements: Deductions for urban boundary layer parameterizations and exchange processes, *Phys. Fluids* 26 (2014), 086603.
- [103] B. Addepalli, E.R. Pardyjak, A study of flow fields in step-down street canyons, *Environ. Fluid Mech.* 15 (2015) 439–481.
- [104] L. Perret, K. Blackman, E. Savory, Combining wind-tunnel and field measurements of street-canyon flow via stochastic estimation, *Boundary-Layer Meteorol.* 161 (2016) 491–517.
- [105] M. Llaguno-Munitxa, E. Bou-Zeid, M. Hultmark, The influence of building geometry on street canyon air flow: validation of large eddy simulations against wind tunnel experiments, *J. Wind Eng. Ind. Aerod.* 165 (2017) 115–130.
- [106] S. Karra, L. Malki-Epshtein, M.K.A. Neophytou, Air flow and pollution in a real, heterogeneous urban street canyon: a field and laboratory study, *Atmos. Environ.* 165 (2017) 370–384.
- [107] Z. Liu, Z. Yu, X. Chen, R. Cao, F. Zhu, An investigation on external airflow around low-rise building with various roof types: PIV measurements and LES simulations, *Build. Environ.* 169 (2020) 106583.
- [108] C. Gromke, R. Buccolieri, S. Di Sabatino, B. Ruck, Dispersion study in a street canyon with tree planting by means of wind tunnel and numerical investigations – evaluation of CFD data with experimental data, *Atmos. Environ.* 42 (2008) 8640–8650.
- [109] Y. Topalar, B. Blocken, B. Maiheu, G.J.F. van Heijst, A review on the CFD analysis of urban microclimate, *Renew. Sustain. Energy Rev.* 80 (2017) 1613–1640.
- [110] M. Vonlanthen, J. Allegrini, J. Carmeliet, Multiscale interaction between a cluster of buildings and the ABL developing over a real terrain, *Urban Climate* 20 (2017) 1–19.
- [111] J. Franke, C. Hirsch, G. Jensen, H.W. Krus, S.D. Miles, M. Schatzmann, N. Wright, Recommendations on the use of CFD in wind engineering, in: Proceedings of the International Conference on Urban Wind Engineering and Building Aerodynamics, 2004. C.1.1–C1.11.
- [112] J. Franke, A. Hellsten, K. Schlünzen, B. Carissimo, Best Practice Guideline for the CFD Simulation of Flows in the Urban Environment, COST Office, Hamburg, 2007.
- [113] Y. Tominaga, A. Mochida, R. Yoshie, H. Kataoka, T. Nozu, M. Yoshikawa, T. Shirasawa, AJI guidelines for practical applications of CFD to pedestrian wind environment around buildings, *J. Wind Eng. Ind. Aerod.* 96 (2008) 1749–1761.
- [114] B. Blocken, Computational Fluid Dynamics for urban physics: Importance, scales, possibilities, limitations and ten tips and tricks towards accurate and reliable simulations, *Build. Environ.* 91 (2015) 219–245.
- [115] B. Blocken, C. Guagliari, Ten iterative steps for model development and evaluation applied to computational fluid dynamics for environmental fluid mechanics, *Environ. Model. Software* 33 (2012) 1–22.
- [116] P.J. Richards, S.E. Norris, Appropriate boundary conditions for computational wind engineering models revisited, *J. Wind Eng. Ind. Aerod.* 99 (2011) 257–266.
- [117] A. Ricci, I. Kalkman, B. Blocken, M. Burlando, M.P. Repetto, Impact of turbulence models and roughness height in 3D steady RANS simulations of wind flow in an urban environment, *Build. Environ.* 171 (2020) 106617.
- [118] M. Schatzmann, S. Rafailidis, M. Pavageau, Some remarks on the validation of small-scale dispersion models with field and laboratory data, *J. Wind Eng. Ind. Aerod.* 67–68 (1997) 885–893.
- [119] M. Schatzmann, B. Leitl, Issues with validation of urban flow and dispersion CFD models, *J. Wind Eng. Ind. Aerod.* 99 (2011) 169–186.
- [120] H.W. Coleman, F. Stern, Uncertainties and CFD code validation, *J. Fluid Eng.* 119 (1997) 795–803.
- [121] Y. Tominaga, T. Stathopoulos, Numerical simulation of dispersion around an isolated cubic building: model evaluation of RANS and LES, *Build. Environ.* 45 (2010) 2231–2239.
- [122] S.M. Salim, R. Buccolieri, A. Chan, S. Di Sabatino, Numerical simulation of atmospheric pollutant dispersion in an urban street canyon: comparison between RANS and LES, *J. Wind Eng. Ind. Aerod.* 99 (2011) 103–113.
- [123] Y. Tominaga, T. Stathopoulos, CFD modeling of pollution dispersion in a street canyon: comparison between LES and RANS, *J. Wind Eng. Ind. Aerod.* 99 (2011) 340–348.
- [124] A. Kubilay, Numerical Simulations and Field Experiments of Wetting of Building Facades Due to Wind-Driven Rain in Urban Areas, Ph.D Thesis, ETH Zurich, 2014.
- [125] B. Blocken, LES over RANS in building simulation for outdoor and indoor applications: A foregone conclusion? *Building Simulation* 11 (2018) 821–870.
- [126] B. Blocken, 50 years of computational wind engineering: past, present and future, *J. Wind Eng. Ind. Aerod.* 129 (2014) 69–102.
- [127] T. Lassila, A. Manzoni, A. Quarteroni, G. Rozza, Model order reduction in fluid dynamics: Challenges and perspectives, in: A. Quarteroni, G. Rozza (Eds.), Reduced Order Methods for Modeling and Computational Reduction, Springer International Publishing, Cham, 2014, pp. 235–273.
- [128] J. Song, S. Fan, W. Lin, L. Mottet, H. Woodward, M. Davies Wykes, R. Arcucci, D. Xiao, J.E. Debay, H. ApSimon, E. Aristodemou, D. Birch, M. Carpenteri, F. Fang, M. Herzog, G.R. Hunt, R.L. Jones, C. Pain, D. Pavlidis, A.G. Robins, C. A. Short, P.F. Linden, Natural ventilation in cities: the implications of fluid mechanics, *Build. Res. Inf.* 46 (2018) 809–828.
- [129] J.S. Peterson, The reduced basis method for incompressible viscous flow calculations, *SIAM J. Sci. Stat. Comput.* 10 (1989) 777–786.
- [130] K. Ito, S.S. Ravindran, A reduced-order method for simulation and control of fluid flows, *J. Comput. Phys.* 143 (1998) 403–425.
- [131] F. Fang, T. Zhang, D. Pavlidis, C.C. Pain, A.G. Buchan, I.M. Navon, Reduced order modelling of an unstructured mesh air pollution model and application in 2D/3D urban street canyons, *Atmos. Environ.* 96 (2014) 96–106.
- [132] L. Vervecken, J. Camps, J. Meyers, Stable reduced-order models for pollutant dispersion in the built environment, *Build. Environ.* 92 (2015) 360–367.
- [133] D. Xiao, F. Fang, C.E. Heaney, I.M. Navon, C.C. Pain, A domain decomposition method for the non-intrusive reduced order modelling of fluid flow, *Comput. Methods Appl. Engng.* 354 (2019) 307–330.
- [134] D. Xiao, C.E. Heaney, L. Mottet, F. Fang, W. Lin, I.M. Navon, Y. Guo, O.K. Matar, A.G. Robins, C.C. Pain, A reduced order model for turbulent flows in the urban environment using machine learning, *Build. Environ.* 148 (2019) 323–337.
- [135] D. Greenspan, Numerical studies of prototype cavity flow problems\*, *Comput. J.* 12 (1969) 88–93.
- [136] C.J. Greenshields, Openfoam User Guide 3, OpenFOAM Found. Ltd Version, 2015, p. e2888, 2015.
- [137] Y. Huang, X. Hu, N. Zeng, Impact of wedge-shaped roofs on airflow and pollutant dispersion inside urban street canyons, *Build. Environ.* 44 (2009) 2335–2347.
- [138] H. Wen, L. Malki-Epshtein, A parametric study of the effect of roof height and morphology on air pollution dispersion in street canyons, *J. Wind Eng. Ind. Aerod.* 175 (2018) 328–341.
- [139] C. Yuan, E. Ng, L.K. Norford, Improving air quality in high-density cities by understanding the relationship between air pollutant dispersion and urban morphologies, *Build. Environ.* 71 (2014) 245–258.

- [140] Y. Tominaga, S.-i. Akabayashi, T. Kitahara, Y. Arinami, Air flow around isolated gable-roof buildings with different roof pitches: wind tunnel experiments and CFD simulations, *Build. Environ.* 84 (2015) 204–213.
- [141] L.W. Chew, L.K. Norford, Pedestrian-level wind speed enhancement in urban street canyons with void decks, *Build. Environ.* 146 (2018) 64–76.
- [142] P.-Y. Cui, Z. Li, W.-Q. Tao, Investigation of Re-independence of turbulent flow and pollutant dispersion in urban street canyon using numerical wind tunnel (NWT) models, *Int. J. Heat Mass Tran.* 79 (2014) 176–188.
- [143] C. Shu, L. Wang, M. Mortezaeezadeh, Dimensional analysis of Reynolds independence and regional critical Reynolds numbers for urban aerodynamics, *J. Wind Eng. Ind. Aerodyn.* 203 (2020) 104232.
- [144] J. Zhong, X.-M. Cai, W.J. Bloss, Modelling the dispersion and transport of reactive pollutants in a deep urban street canyon: using large-eddy simulation, *Environ. Pollut.* 200 (2015) 42–52.
- [145] L. He, J. Hang, X. Wang, B. Lin, X. Li, G. Lan, Numerical investigations of flow and passive pollutant exposure in high-rise deep street canyons with various street aspect ratios and viaduct settings, *Sci. Total Environ.* 584–585 (2017) 189–206.
- [146] L.W. Chew, A.A. Aliabadi, L.K. Norford, Airflows in narrow street canyons: single or double vortex?, in: Proceedings of the 2019 CSME International Congress, June 2–5, 2019, 2019, Ontario, Canada.
- [147] J. Hang, X. Chen, G. Chen, T. Chen, Y. Lin, Z. Luo, X. Zhang, Q. Wang, The Influence of Aspect Ratios and Wall Heating Conditions on Flow and Passive Pollutant Exposure in 2D Typical Street Canyons, *Building and Environment*, 2019, p. 106536.
- [148] K. Zhang, G. Chen, X. Wang, S. Liu, C.M. Mak, Y. Fan, J. Hang, Numerical evaluations of urban design technique to reduce vehicular personal intake fraction in deep street canyons, *Sci. Total Environ.* 653 (2019) 968–994.
- [149] L.W. Chew, N. Nazarian, L. Norford, Pedestrian-level urban wind flow enhancement with wind catchers, *Atmosphere* 8 (2017) 159.
- [150] B. Blocken, T. Stathopoulos, J. Carmeliet, CFD simulation of the atmospheric boundary layer: wall function problems, *Atmos. Environ.* 41 (2007) 238–252.
- [151] D.M. Hargreaves, N.G. Wright, On the use of the k-e model in commercial CFD software to model the neutral atmospheric boundary layer, *J. Wind Eng. Ind. Aerodyn.* 95 (2007) 355–369.
- [152] B. Blocken, J. Persoon, Pedestrian wind comfort around a large football stadium in an urban environment: CFD simulation, validation and application of the new Dutch wind nuisance standard, *J. Wind Eng. Ind. Aerodyn.* 97 (2009) 255–270.
- [153] W.D. Janssen, B. Blocken, T. van Hooff, Pedestrian wind comfort around buildings: comparison of wind comfort criteria based on whole-flow field data for a complex case study, *Build. Environ.* 59 (2013) 547–562.
- [154] R.N. Meroney, Wind Tunnel and Numerical Simulation of Pollution Dispersion: A Hybrid Approach. Invited Lecture, Croucher Advanced Study Institute, Hong University of Science and Technology, 2004, 6–10 December 2004.
- [155] R.N. Meroney, Ten questions concerning hybrid computational/physical model simulation of wind flow in the built environment, *Build. Environ.* 96 (2016) 12–21.
- [156] W.H. Snyder, Similarity criteria for the application of fluid models to the study of air pollution meteorology, *Boundary-Layer Meteorol.* 3 (1972) 113–134.
- [157] R. Davy, I. Esau, Differences in the efficacy of climate forcings explained by variations in atmospheric boundary layer depth, *Nat. Commun.* 7 (2016) 11690.
- [158] A. Jericević, B. Grisogono, The critical bulk Richardson number in urban areas: verification and application in a numerical weather prediction model, *Tellus Dyn. Meteorol. Oceanogr.* 58 (2006) 19–27.
- [159] P.-Y. Cui, Z. Li, W.-Q. Tao, Buoyancy flows and pollutant dispersion through different scale urban areas: CFD simulations and wind-tunnel measurements, *Build. Environ.* 104 (2016) 76–91.
- [160] A.J. Wells, M.G. Worster, A geophysical-scale model of vertical natural convection boundary layers, *J. Fluid Mech.* 609 (2008) 111–137.
- [161] S.-B. Park, J.-J. Baik, S. Raasch, M.O. Letzel, A large-eddy simulation study of thermal effects on turbulent flow and dispersion in and above a street canyon, *J. Appl. Meteorol. Climatol.* 51 (2012) 829–841.
- [162] M. Santamouris, N. Papаниkolaou, I. Koronakis, I. Livada, D. Asimakopoulos, Thermal and air flow characteristics in a deep pedestrian canyon under hot weather conditions, *Atmos. Environ.* 33 (1999) 4503–4521.
- [163] C.A. Bilton, Customer Report for Mock Urban Setting Test (MUST). DTC Project No. 8-CO-160-000-052, 2001.
- [164] M.W. Rotach, R. Vogt, C. Bernhofer, E. Batchvarova, A. Christen, A. Clappier, B. Feddersen, S.E. Gryning, G. Martucci, H. Mayer, V. Mitev, T.R. Oke, E. Parlow, H. Richner, M. Roth, Y.A. Roulet, D. Ruffieux, J.A. Salmon, M. Schatzmann, J. A. Voogt, Bubble – an urban boundary layer meteorology project, *Theor. Appl. Climatol.* 81 (2005) 231–261.
- [165] B. Offerle, I. Eliasson, C.S.B. Grimmond, B. Holmer, Surface heating in relation to air temperature, wind and turbulence in an urban street canyon, *Boundary-Layer Meteorol.* 122 (2007) 273–292.
- [166] M. Idczak, P. Mestayer, J.-M. Rosant, J.-F. Sini, M. Violleau, Micrometeorological measurements in a street canyon during the joint ATREUS-PICADA experiment, *Boundary-Layer Meteorol.* 124 (2007) 25–41.
- [167] I. Kanda, Y. Yamao, Passive scalar diffusion in and above urban-like roughness under weakly stable and unstable thermal stratification conditions, *J. Wind Eng. Ind. Aerod.* 148 (2016) 18–33.
- [168] Y. Lin, T. Ichinose, Y. Yamao, H. Mouri, Wind velocity and temperature fields under different surface heating conditions in a street canyon in wind tunnel experiments, *Build. Environ.* 168 (2020) 106500.
- [169] R.E. Britter, S.R. Hanna, Flow and dispersion IN urban areas, *Annu. Rev. Fluid Mech.* 35 (2003) 469–496.
- [170] P. Klein, J.V. Clark, Flow variability in a north American downtown street canyon, *J. Appl. Meteorol. Climatol.* 46 (2007) 851–877.
- [171] A.A. Balogun, A.S. Tomlin, C.R. Wood, J.F. Barlow, S.E. Belcher, R.J. Smalley, J.J. N. Lingard, S.J. Arnold, A. Dobre, A.G. Robins, D. Martin, D.E. Shallcross, In-street wind direction variability in the vicinity of a busy intersection in central London, *Boundary-Layer Meteorol.* 136 (2010) 489–513.
- [172] X. Xie, C.-H. Liu, D.Y.C. Leung, Impact of building facades and ground heating on wind flow and pollutant transport in street canyons, *Atmos. Environ.* 41 (2007) 9030–9049.
- [173] N. Antoniou, H. Montazeri, M. Neophytou, B. Blocken, CFD simulation of urban microclimate: Validation using high-resolution field measurements, *Sci. Total Environ.* 695 (2019) 133743.
- [174] J. Ke, N. Williamson, S.W. Armfield, G.D. McBain, S.E. Norris, Stability of a temporally evolving natural convection boundary layer on an isothermal wall, *J. Fluid Mech.* 877 (2019) 1163–1185.
- [175] Y. Zhao, P. Zhao, Y. Liu, Y. Xu, J.F. Torres, On the selection of perturbations for thermal boundary layer control, *Phys. Fluids* 31 (2019) 104102.
- [176] J. Kong, J. Niu, C. Lei, A CFD based approach for determining the optimum inclination angle of a roof-top solar chimney for building ventilation, *Sol. Energy* 198 (2020) 555–569.
- [177] P.J. Richards, R.P. Hoxey, Appropriate boundary conditions for computational wind engineering models using the k-e turbulence model, *J. Wind Eng. Ind. Aerod.* 46–47 (1993) 145–153.
- [178] Y. Toparlar, B. Blocken, B. Maiheu, G. van Heijst, CFD simulation of the near-neutral atmospheric boundary layer: New temperature inlet profile consistent with wall functions, *J. Wind Eng. Ind. Aerod.* 191 (2019) 91–102.
- [179] J. Allegrini, V. Dorer, J. Carmeliet, Buoyant flows in street canyons: Validation of CFD simulations with wind tunnel measurements, *Build. Environ.* 72 (2014) 63–74.
- [180] T. Defraeye, B. Blocken, J. Carmeliet, CFD analysis of convective heat transfer at the surfaces of a cube immersed in a turbulent boundary layer, *Int. J. Heat Mass Tran.* 53 (2010) 297–308.
- [181] B.E. Launder, D.B. Spalding, The numerical computation of turbulent flows, *Comput. Meth. Appl. Engng.* 3 (1974) 269–289.
- [182] T. Defraeye, B. Blocken, J. Carmeliet, CFD simulation of heat transfer at surfaces of bluff bodies in turbulent boundary layers: Evaluation of a forced-convective temperature wall function for mixed convection, *J. Wind Eng. Ind. Aerod.* 104–106 (2012) 439–446.
- [183] J. Allegrini, V. Dorer, T. Defraeye, J. Carmeliet, An adaptive temperature wall function for mixed convective flows at exterior surfaces of buildings in street canyons, *Build. Environ.* 49 (2012) 55–66.
- [184] J. Allegrini, V. Dorer, J. Carmeliet, Analysis of convective heat transfer at building façades in street canyons and its influence on the predictions of space cooling demand in buildings, *J. Wind Eng. Ind. Aerod.* 104–106 (2012) 464–473.
- [185] B. Blocken, T. Defraeye, D. Derome, J. Carmeliet, High-resolution CFD simulations for forced convective heat transfer coefficients at the facade of a low-rise building, *Build. Environ.* 44 (2009) 2396–2412.
- [186] J. Allegrini, V. Dorer, J. Carmeliet, Coupled CFD, radiation and building energy model for studying heat fluxes in an urban environment with generic building configurations, *Sustainable Cities and Society* 19 (2015) 385–394.
- [187] S. Bottillo, A. De Lieto Vollaro, G. Galli, A. Vallati, Fluid dynamics and heat transfer parameters in an urban canyon, *Sol. Energy* 99 (2014) 1–10.
- [188] M.-Y. Tsai, K.-S. Chen, C.-H. Wu, Three-dimensional modeling of air flow and pollutant dispersion in an urban street canyon with thermal effects, *J. Air Waste Manag. Assoc.* 55 (2005) 1178–1189.
- [189] N. Nazarian, J. Kleissl, CFD simulation of an idealized urban environment: Thermal effects of geometrical characteristics and surface materials, *Urban Climate* 12 (2015) 141–159.
- [190] M.L. Shur, P.R. Spalart, M.K. Strelets, A.K. Travin, A hybrid RANS-LES approach with delayed-DES and wall-modelled LES capabilities, *Int. J. Heat Fluid Flow* 29 (2008) 1638–1649.
- [191] S. Kenjeres, K. Hanjalić, LES, T-RANS and hybrid simulations of thermal convection at high Ra numbers, *Int. J. Heat Fluid Flow* 27 (2006) 800–810.
- [192] K. Hanjalić, M. Hrebto, Ground boundary conditions for thermal convection over horizontal surfaces at high Rayleigh numbers, *Boundary-Layer Meteorol.* 160 (2016) 41–61.
- [193] M. Hrebto, K. Hanjalić, Numerical study of winter diurnal convection over the city of krasnoyarsk: Effects of non-freezing river, undulating fog and steam devils, *Boundary-Layer Meteorol.* 163 (2017) 469–495.
- [194] T. Tsuji, Y. Nagano, Characteristics of a turbulent natural convection boundary layer along a vertical flat plate, *Int. J. Heat Mass Tran.* 31 (1988) 1723–1734.
- [195] Z.-T. Xie, P. Hayden, C.R. Wood, Large-eddy simulation of approaching-flow stratification on dispersion over arrays of buildings, *Atmos. Environ.* 71 (2013) 64–74.
- [196] D. Marucci, M. Carpentieri, P. Hayden, On the simulation of thick non-neutral boundary layers for urban studies in a wind tunnel, *Int. J. Heat Fluid Flow* 72 (2018) 37–51.
- [197] D. Marucci, M. Carpentieri, Dispersion in an array of buildings in stable and convective atmospheric conditions, *Atmos. Environ.* 222 (2020) 117100.
- [198] V. Sessa, Z.-T. Xie, S. Herring, Thermal stratification effects on turbulence and dispersion in internal and external boundary layers, *Boundary-Layer Meteorol.* 176 (2020) 61–83.
- [199] G. Duan, K. Ngan, Sensitivity of turbulent flow around a 3-D building array to urban boundary-layer stability, *J. Wind Eng. Ind. Aerod.* 193 (2019) 103958.

- [200] A.C. Rudd, A.G. Robins, J.J. Lepley, S.E. Belcher, An inverse method for determining source characteristics for emergency response applications, *Boundary-Layer Meteorol.* 144 (2012) 1–20.
- [201] S.E. Belcher, O. Coceal, E.V. Goulart, A.C. Rudd, A.G. Robins, Processes controlling atmospheric dispersion through city centres, *J. Fluid Mech.* 763 (2015) 51–81.
- [202] A. Tzella, J. Vanneste, Dispersion in rectangular networks: effective diffusivity and large-deviation rate function, *Phys. Rev. Lett.* 117 (2016) 114501.
- [203] Y. Lee, B. Engquist, Multiscale numerical methods for passive advection-diffusion in incompressible turbulent flow fields, *J. Comput. Phys.* 317 (2016) 33–46.
- [204] K.W. Lo, K. Ngan, Multiscale parameterisation of passive scalars via wavelet-based numerical homogenisation, *Appl. Math. Model.* 82 (2020) 217–234.
- [205] J. Hang, Y. Li, Wind conditions in idealized building clusters: macroscopic simulations using a porous turbulence model, *Boundary-Layer Meteorol.* 136 (2010) 129–159.
- [206] J. Hang, Y. Li, Macroscopic simulations of turbulent flows through high-rise building arrays using a porous turbulence model, *Build. Environ.* 49 (2012) 41–54.
- [207] F.J. Valdés-Parada, C.G. Aguilar-Madera, J.A. Ochoa-Tapia, B. Goyeau, Velocity and stress jump conditions between a porous medium and a fluid, *Adv. Water Resour.* 62 (2013) 327–339.
- [208] X. Wang, Y. Li, J. Hang, A combined fully-resolved and porous approach for building cluster wind flows, *Building Simulation* 10 (2017) 97–109.
- [209] X. Wang, Y. Li, Predicting urban heat island circulation using CFD, *Build. Environ.* 99 (2016) 82–97.